THE JOURNAL OF BIOLOGICAL CHEMISTRY VOL. 290, NO. 1, pp. 505–519, January 2, 2015

O-Fucose Monosaccharide of *Drosophila* Notch Has a Temperature-sensitive Function and Cooperates with *O*-Glucose Glycan in Notch Transport and Notch Signaling Activation*

Received for publication, October 4, 2014 Published, JBC Papers in Press, November 5, 2014, DOI 10.1074/jbc.M114.616847

Akira Ishio[‡§1], Takeshi Sasamura[§1], Tomonori Ayukawa[‡], Junpei Kuroda[§], Hiroyuki O. Ishikawa[¶‖], Naoki Aoyama[‡], Kenjiroo Matsumoto[§], Takuma Gushiken[‡§], Tetsuya Okajima[**], Tomoko Yamakawa[§], and Kenji Matsuno[§2]

*From the [‡]Department of Biological Science and Technology, Tokyo University of Science, 6-3-1 Niijuku, Katsushika-ku, Tokyo, 125-1500, the [§]Department of Biological Sciences, Graduate School of Science, Osaka University, 1-1 Machikaneyama, Toyonaka, Osaka 560-0043, [¶]Genome and Drug Research Center, Tokyo University of Science, 2641 Yamazaki, Noda, Chiba, 278-8510, the [‖]Graduate School of Science,Chiba University, 1-33 Yayoi, Inage, Chiba, and the **Department of Biochemistry II, Nagoya University Graduate School of Medicine, Tsurumai, Showa-ku, Nagoya 466-0065, Japan*

Background: The requirement of *O*-fucose monosaccharide on Notch is not fully understood.
Results: Loss of *O*-fucose monosaccharide on Notch caused temperature-sensitive loss of Notch signaling.
Conclusion: *O*-Fucose monosaccharide of Notch has a temperature-sensitive function and cooperates with *O*-glucose glycan in Notch signal activation.
Significance: Our findings elucidate how different forms of glycosylation on a protein influence protein functions.

Notch (N) is a transmembrane receptor that mediates the cell-cell interactions necessary for many cell fate decisions. N has many epidermal growth factor-like repeats that are *O*-fucosylated by the protein *O*-fucosyltransferase 1 (*O*-Fut1), and the *O-fut1* gene is essential for N signaling. However, the role of the monosaccharide *O*-fucose on N is unclear, because *O*-Fut1 also appears to have *O*-fucosyltransferase activity-independent functions, including as an N-specific chaperon. Such an enzymatic activity-independent function could account for the essential role of *O-fut1* in N signaling. To evaluate the role of the monosaccharide *O*-fucose modification in N signaling, here we generated a knock-in mutant of *O-fut1* (*O-fut1*$^{R245A\ knock\text{-}in}$), which expresses a mutant protein that lacks *O*-fucosyltransferase activity but maintains the N-specific chaperon activity. Using *O-fut1*$^{R245A\ knock\text{-}in}$ and other gene mutations that abolish the *O*-fucosylation of N, we found that the monosaccharide *O*-fucose modification of N has a temperature-sensitive function that is essential for N signaling. The *O*-fucose monosaccharide and *O*-glucose glycan modification, catalyzed by Rumi, function redundantly in the activation of N signaling. We also showed that the redundant function of these two modifications is responsible for the presence of N at the cell surface. Our findings elucidate how different forms of glycosylation on a protein can influence the protein's functions.

Cell-cell signaling mediated by Notch (N)[3] receptors plays crucial roles in many developmental processes in multicellular organisms (1–4). In humans, aberrant N signaling causes or is implicated in numerous diseases, including Alagille syndrome, spondylocostal dysostosis, cerebral autosomal dominant arteriopathy with subcortical infarcts and leukoencephalopathy, multiple sclerosis, and various cancers (5–7).

N receptor family proteins have multiple EGF-like repeats in their extracellular domain (1–4), many of which can be modified with several types of *O*-linked glycosylation: *O*-fucose, *O*-glucose, *O*-xylose, and *O*-GlcNAc (8–12). N is *O*-fucosylated at serine or threonine residues in the $C^2XXXX(S/T)C^3$ consensus sequence that is present in various EGF-like repeats; for example, *Drosophila* has 36 EGF-like repeats, 23 of which are *O*-fucosylated (8, 13). This modification is mediated by protein *O*-fucosyltransferase 1 (*O*-Fut1 in *Drosophila* and protein *O*-fucosyltransferase 1 in mammals). β1,3-GlcNAc is further added to the *O*-fucose residue by Fringe (Fng) family proteins, which are β1,3-*N*-acetylglucosaminyltransferases (14, 15).

O-fut1 and *Pofut1* are apparently globally required for normal N signaling in *Drosophila* and mammals, respectively, in that their mutant phenotypes are similar to those caused by disrupted N signaling (16–18). In contrast, mutants of genes encoding Fng family proteins reduce N signaling in only a subset of contexts that involve N signaling (15, 19–21). Therefore, the GlcNAc modification by Fng, which regulates the interaction between N and its ligands, Delta (Dl) or Serrate, is required in a tissue-specific manner for various tissue boundary formations (22).

* This work was supported by grants-in-aid from the Japanese Ministry of Education, Culture, Sports and Science (to K. M. and T. A.) and grants from PRESTO, Japan Science and Technology Agency (to K. M.).
[1] Both authors contributed equally to this work.
[2] To whom correspondence should be addressed. Tel.: 81-6-6850-5804; Fax: 81-6-6850-5805; E-mail: kmatsuno@bio.sci.osaka-u.ac.jp.
[3] The abbreviations used are: N, Notch; dpp, decapentaplegic; *D*E-Cad, *D*E-cadherin; Dl, Delta; D/V, dorsal and ventral; ER, endoplasmic reticulum; Fng, Fringe; Gmer, GDP-4 keto-6 deoxy-D-mannose epimerase/reductase; Gmd, GDP-mannose 4,6-dehydratase; m/z, maternal and zygotic; $N^{\Delta E}$, a membrane-tethered form of activated Notch; N^{FL}, full-length Notch; NICD, Notch intracellular domain; *O*-Fut1, *O*-fucosyltransferase 1; Sens, Senseless; SOP, sensory organ precursor; Wg, Wingless; MARCM, mosaic analysis with a repressible cell marker.

O-Fut1 has two *O*-fucosyltransferase activity-independent functions (23–26). First, it is an endoplasmic reticulum (ER) resident protein and functions as a N-specific chaperon (23). Second, overexpressed *O*-Fut1 promotes the endocytosis of the N cell nonautonomously (25). Thus, it has been difficult to determine whether *O*-Fut1's *O*-fucosyltransferase activity or its nonenzymatic functions (or both) are required in N signaling. To address this issue, Okajima *et al.* (23) generated a genomic fragment, including a mutant *O-fut1* locus, *O-fut1*^{R245A}, which produces an *O*-Fut1 variant carrying an amino acid substitution in the binding site for GDP-fucose. *O*-Fut1^{R245A} lacks *O*-fucosyltransferase activity *in vitro*, although it reportedly retains its N-specific chaperon activity (23). Most of the defects associated with the absence of *O-fut1* are rescued by introducing the *O-fut1*^{R245A} genomic locus, except for the phenotypes that are probably due to the disruption of Fng functions, which are tissue-specific and depend on the *O*-fucosylation of N (24). Based on these results, it was proposed that the *O*-fucose monosaccharide modification of N does not have a specific function in N signaling, although it is required for the Fng-dependent activation of N signaling. However, it was also reported that the ability of the *O-fut1*^{R245A} genomic locus to rescue the *O-fut1* null allele differs among transgenic lines, probably because the insertion site of the transgene affects the transcription efficiency of the integrated *O-fut1*^{R245A} locus (23, 24).

To overcome this problem, here we generated a knock-in mutant of *O-fut1*^{R245A} (*O-fut1*$^{R245A\ knock\text{-}in}$) in *Drosophila melanogaster*. We used *O-fut1*$^{R245A\ knock\text{-}in}$ and other mutants affecting the *O*-fucosylation of Notch's EGF-like repeats to examine the specific role of the monosaccharide *O*-fucose in N signaling. We also studied the genetic interaction between *O-fut1*$^{R245A\ knock\text{-}in}$ and *rumi*, which encodes an *O*-glucosyltransferase that adds *O*-glucose to the EGF-like repeats of N (27–30). Based on the presented results, we propose a model showing how multiple *O*-glycosylation sites in EGF-like repeats might affect the function of N.

EXPERIMENTAL PROCEDURES

Drosophila Strains—Canton-S was used as the wild-type strain. The following mutant alleles were used: *O-fut1*^{4R6}, a null allele (17); *fng*^{13}, a strong loss-of-function allele (31); *Gmd*^{H78}, a null allele (25); *Gmer*^{SH} *l(2)SH1931*, a P-element insertion allele (32, 33); Df(2R)BSC783, a deficiency uncovering the *Gmer* locus (33); and *rumi*^{44}, a null allele (27). The following UAS lines were used: *UAS-N*^{FL} (a gift from S. Artavanis-Tsakonas), *UAS-N*$^{\Delta E}$ (34), *UAS-NICD* (35), and *UAS-Lamp-HRP* (36). Decapentaplegic (*dpp*)-*Gal4* was described previously (37). *2xUbx-FLP* was used to efficiently induce somatic mosaic clones (38). To induce germ line mosaic clones, *ovo*^{D} *G13* (17), *ovo*^{D} *FRT40A*, and *ovo*^{D} *FRT80B* (39) were used.

Generation of the O-fut1$^{R245A\ knock\text{-}in}$ *Fly*—*O-fut1*$^{R245A\ knock\text{-}in}$ is a knock-in mutation generated by a homologous recombination method described previously (40, 41). Two genomic fragments covering the *O-fut1* locus, referred to as the left arm and right arm, were PCR-amplified. The left arm (5005 bp) was amplified using the primers 5′-CAACCAAGCAGGGCCAATCCCA-3′ and 5′-AATTTCTTATAGTCATATAAATACAAAATA-3′, and it included the region from 4560 bp upstream of the start of the *O-fut1* 5′UTR to 188 bp downstream of the end of the *O-fut1* 3′UTR. The right arm (4996 bp) was amplified using the primers 5′-TCTTTTAGCTTTAATTCTTAAAAAGGATTT-3′ and 5′-CCGAATCGGCGACCCAGTAAAC-3′, and it included the region from 189 bp downstream of the end of the *O-fut1* 3′UTR to 5115-bp downstream of the end of the *O-fut1* 3′UTR. The left arm fragment was inserted into the AscI site of the pT7 Blue vector (Novagen), and the right arm fragment was inserted between the SphI and NotI sites of the pT7 Blue vector. The resulting constructs were pT7 Blue+left arm and pT7 Blue+right arm. To introduce a base substitution that would result in the amino acid replacement of arginine (Arg) at the 245th amino acid with alanine (Ala), an overlap extension PCR was performed using pT7 Blue+left arm and two primers, 5′-CATCTGGCCAACGGTATCGATTGGGTG-3′ and 5′-ACCGTTGGCCAGATGAATGCCCAAAAA3′. The right arm and mutated left arm were excised and cloned into an ends-out homologous recombination vector, pW25, with a selectable marker, *white* (40, 41). This construct was introduced into the *Drosophila* genome by P-element-mediated transformation (41). Using the transgenic line obtained, homologous recombination was performed as described previously (40, 41). Briefly, pW25 contains two lox sites, which make it feasible to remove the *white* marker by Cre-mediated recombination (41). The *white* marker was removed as described previously (41), and the resulting lines were maintained as *O-fut1*$^{R245A\ knock\text{-}in}$. The *O-fut1* locus of the *O-fut1*$^{R245A\ knock\text{-}in}$ line was sequenced, and the mutation was confirmed.

Generation of Somatic Mosaic Clones—Somatic clones of *O-fut1*$^{R245A\ knock\text{-}in}$ and *fng*^{13} were generated by mitotic recombination in wing discs isolated from the larvae of *y w 2×Ubx-FLP*; *FRTG13 O-fut1*$^{R245A\ knock\text{-}in}$*/FRTG13 Ubi-GFP* and *y w 2×Ubx-FLP*; *fng*^{13} *FRT80B/Ubi-GFP FRT80B*, *y w 2×Ubx-FLP*; *FRT82B rumi*^{44}*/FRT82B Ubi-GFP*, *y w 2×Ubx-FLP*; *FRTG13 O-fut1*$^{R245A\ knock\text{-}in}$*/FRTG13 Ubi-GFP*; *FRT82B rumi*^{44}*/FRT82B rumi*^{44}, using the FLP/FRT system, as described before (42). To express *UAS-Lamp-HRP* in wild-type or *O-fut1*$^{R245A\ knock\text{-}in}$ mutants, the following males were crossed to *2×Ubx-FLP*; *FRTG13 tub-Gal80/CyO*; *tub-Gal4/TM6B* females, respectively: *FRTG13*; *UAS-Lamp-HRP/TM6B,* and *FRTG13 O-fut1*$^{R245A\ knock\text{-}in}$*/CyO*; *UAS-Lamp-HRP/TM6B.* Until the larval stage, cultures were maintained at the indicated temperature (18, 25, or 30 °C).

Epistasis Analysis Involving O-fut1$^{R245A\ knock\text{-}in}$ *and Various N Derivatives Using the MARCM System*—The MARCM system was described previously (43). The following males were crossed to *2×Ubx-FLP*; *FRTG13 tub-Gal80/CyO*; *tub-Gal4, UAS-GFP/TM6B* females to obtain flies with MARCM clones: *FRTG13 O-fut1*$^{R245A\ knock\text{-}in}$*/CyO*; *UAS-N*^{FL}*/TM6B, FRTG13/CyO*; *UAS-N*^{FL}*/TM6B, FRTG13 O-fut1*$^{R245A\ knock\text{-}in}$*/CyO*; *UAS-N*$^{\Delta E}$*/TM6B, FRTG13/CyO*; *UAS-N*$^{\Delta E}$*/TM6B, FRTG13 O-fut1*$^{R245A\ knock\text{-}in}$*/CyO*; *UAS-NICD/TM6B, FRTG13/CyO*; *UAS-NICD/TM6B.*

Generation of Germ Line Mosaic Clones to Remove the Maternal Contribution—To obtain embryos homozygous for *O-fut1*$^{R245A\ knock\text{-}in}$ that originated from an *O-fut1*$^{R245A\ knock\text{-}in}$ homozygous germ line, *y w hs-FLP/+*; *FRTG13 ovo*^{D}*/FRTG13 O-fut1*$^{R245A\ knock\text{-}in}$ females were crossed with *FRTG13*

O-fut1$^{R245A\ knock\text{-}in}$*/CyO, wg-lacZ* males. To obtain embryos homozygous for *Gmd* and lacking its maternal contribution, *y w hs-FLP/+*; *ovo*^{D} *FRT40A/Gmd*^{H78} *FRT40A* females were crossed with *Gmd*^{H78} *FRT40A/CyO, wg-lacZ* males. To obtain embryos homozygous for *Gmer* and lacking its maternal contribution, *y w hs-FLP/+*; *FRTG13 ovo*^{D}*/FRTG13 Gmer*^{SH} females were crossed with *FRTG13 Gmer*^{SH}*/CyO, wg-lacZ* males. To obtain embryos homozygous for *fng* and lacking its maternal contribution, *y w hs-FLP/+*; *ovo*^{D} *FRT80B/fng*^{13} *FRT80B females were crossed with fng*^{13} *FRT80B/TM3, ftz-lacZ* males. To generate germ line mosaic clones, larvae were heat-shocked at 37 °C for 1 h 48–72 h after egg laying.

Western Blots—Western blotting was performed using a standard protocol (44). Wing discs of third-instar larvae were dissected and homogenized to prepare protein extracts. To detect Notch protein, 30 μg of protein extracts were resolved by electrophoresis on 4–15% Criterion TGX precast gels (Bio-Rad), and an anti-Notch intracellular domain antibody (1:5000 dilution, C17.9C6) (45) was used. As a loading control, α-tubulin was detected with an anti-α-tubulin antibody (1:2000 dilution, DM1A, Sigma) (46).

Immunostaining—Dissections and staining were performed using standard methods (44). The following antibodies were used: mouse anti-Notch intracellular domain (1:500; C17.9C6) (45); mouse anti-Notch extracellular domain (1:500, C458.2H) (47); mouse anti-Wg (1:250; 4D4) (48); mouse anti-Cut (1:250; 2B10) (49); rabbit anti-GFP (1:1,000; MBL, Nagoya, Japan); rat anti-GFP (1:1,000; Nacalai, Kyoto, Japan); rat anti-Elav (50) (1:25, 9F8A9); rabbit anti-Rab7 (1:5,000) (51); rabbit anti-Rab11 (1:10,000) (51); mouse anti-Pdi (1:500, 1D3, EnzoLife Sciences) (52); guinea pig anti-Senseless (1:500) (53); guinea pig anti-Hrs (36); guinea pig anti-*O*-Fut1 (1:1000) (23); and guinea pig anti-Boca (1:500) (54). Cy3-, Cy5-, and Alexa488-coupled secondary antibodies (1:500) were from Jackson ImmunoResearch and Molecular Probes. Images were acquired on an LSM5 Pascal or LSM700 microscope (Zeiss). All images were processed and assembled using ImageJ, Adobe Photoshop, and Adobe Illustrator.

Comparison of the O-Fucose and O-Glucose Sites in Various Notch Receptors—The Swiss-Prot and KEGG GENES databases were searched using the Motif search program or EGF-like repeats containing the consensus sequence for *O*-glucosylation between the first and second cysteines, and for *O*-fucosylation between the second and third cysteines (8, 13).

RESULTS

O-Fucosyltransferase Activity of O-fut1$^{R245A\ knock\text{-}in}$ *Is Negligible in Vivo*—In the previously reported *Drosophila O-fut1*^{R245A} mutant, arginine is replaced by alanine at the 245th amino acid position of the deduced *O*-Fut1 protein (Fig. 1*A*) (23). This amino acid substitution is located in the GDP-fucose-binding motif and largely abolishes the *O*-fucosyltransferase activity *in vitro* (Fig. 1*A*) (23, 55, 56). We first sought to confirm that the *O*-fucosyltransferase activity of *O-fut1*$^{R245A\ knock\text{-}in}$ was also negligible *in vivo*. *O-fut1*$^{R245A\ knock\text{-}in}$ homozygotes survived until the third-instar larval stage (data not shown). In the wild-type wing discs of the third-instar larvae, N signaling is activated at the border between *fng*-expressing and *fng*-nonexpressing regions, which correspond to the dorsal and ventral (D/V) compartments, respectively. Therefore, the expression of *wingless* (*wg*), a downstream gene of N signaling, is activated along the D/V compartment boundary (D/V boundary) (Fig. 1*B*) (57). This activation of N signaling depends on the selective binding of N with Dl or Serrate, which is regulated by GlcNAc

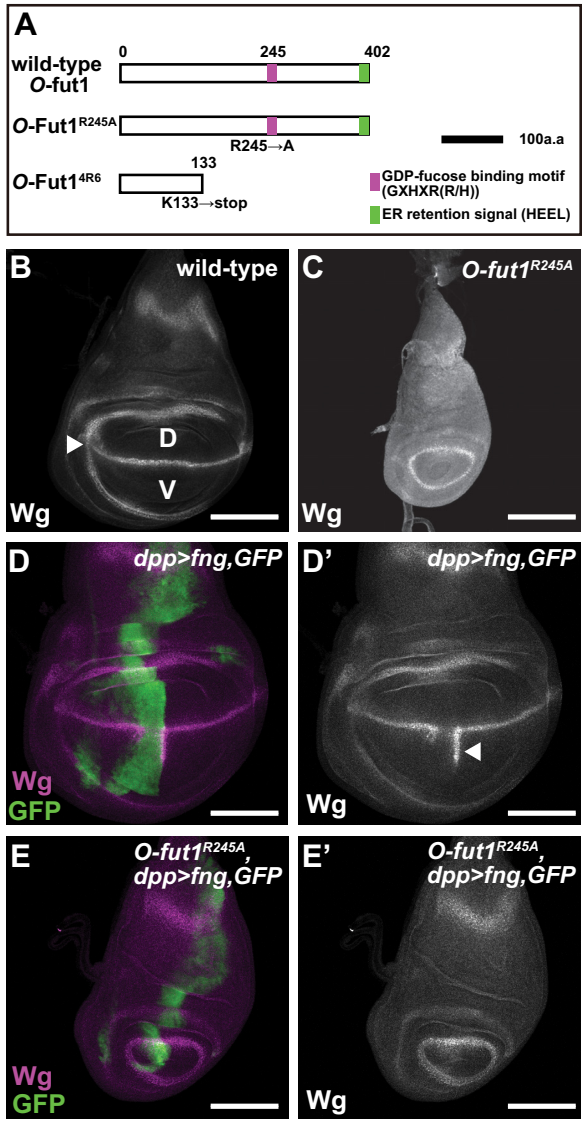

FIGURE 1. ***O*-Fucosyltransferase activity of *O-fut1*$^{R245A\ knock\text{-}in}$ is negligible *in vivo*.** *A*, schematic of the *O*-Fut1 protein and its mutant derivatives. The GDP-fucose-binding motif (G*X*H*X*R(R/H)) and ER retention signal (HEEL) are shown in *magenta* and *green*, respectively. *Top, middle,* and *bottom bars* represent wild-type, *O*-Fut1^{R245A}, and *O*-Fut1^{4R6}, respectively. *O*-Fut1^{R245A} has an amino acid substitution (Arg to Ala) at the 245th amino acid that disrupts its *O*-fucosyltransferase activity. *O-fut1*^{4R6} carries a nonsense mutation that introduces a premature stop codon at the 133rd amino acid. *Black bar* corresponds to 100 amino acids. *B* and *C*, wild-type (*B*) and *O-fut1*$^{R245A\ knock\text{-}in}$ homozygote (*C*) wing discs of third-instar larvae were stained with an anti-Wg antibody. The expression of *wg* along the D/V boundary, which depends on N signaling, is indicated by an *arrowhead* in *B*. *D*, dorsal compartment; *V*, ventral compartment. *D–E′*, *UAS-fng* was misexpressed under the control of *dpp-Gal4* along the anterior-posterior boundary of wild-type (*D* and *D′*) and *O-fut1*$^{R245A\ knock\text{-}in}$ homozygote wing discs (*E* and *E′*). These wing discs were stained with an anti-Wg antibody (*magenta* in *D* and *E* and *white* in *D′* and *E′*). The expression pattern of *dpp-Gal4* was monitored by detecting the *UAS-GFP* expression using an anti-GFP antibody (*green* in *D* and *E*). *D′* and *E′* are single channel images of the *magenta* (anti-Wg staining) in *D* and *E*, respectively. The ectopic expression of *wg* is indicated by an *arrowhead* in *D′*. *Scale bars, B–E′* are 100 μm.

modification of the *O*-fucose on N′s EGF-like repeats by Fng (20). We found that *wg* expression was abolished in the wing discs isolated from *O-fut1*$^{R245A\ knock\text{-}in}$ homozygotes at the third instar cultured at 25 °C (Fig. 1*C*), probably because the *fng* function was disrupted in the absence of N′s *O*-fucosylation.

As reported previously, misexpressed *fng* driven by *dpp-Gal4* at 25 °C resulted in the ectopic activation of *wg* in the ventral compartment of the wild-type wing, where endogenous *fng* is not expressed ($n = 99$) (Fig. 1, *D* and *D*′). However, when we misexpressed *fng* driven by *dpp-Gal4* in the wing discs of *O-fut1*$^{R245A\ knock\text{-}in}$ homozygotes cultured at 25 °C, no *wg* expression was induced in any case examined ($n = 52$) (Fig. 1, *E* and *E*′). We confirmed that the expression pattern of *dpp-Gal4* was almost the same in the wing discs of wild-type and *O-fut1*$^{R245A\ knock\text{-}in}$ homozygotes at this temperature (Fig. 1, *D* and *E*). This result suggested that in the *O-fut1*$^{R245A\ knock\text{-}in}$ homozygotes, the *O*-fucose modification of N was minimal, if it occurred at all.

O-fut1 is a maternal-effect gene (17). Therefore, to observe the phenotypes associated with the *O-fut1*$^{R245A\ knock\text{-}in}$ mutation, we needed to remove the maternal contribution of the wild-type *O-fut1* gene from the female germ line. However, these females are heterozygous for *O-fut1*$^{R245A\ knock\text{-}in}$, because *O-fut1*$^{R245A\ knock\text{-}in}$ is a recessive lethal mutation (data not shown). Therefore, we obtained embryos homozygous for *O-fut1*$^{R245A\ knock\text{-}in}$ from females carrying germ line clones homozygous for *O-fut1*$^{R245A\ knock\text{-}in}$, using a previously described method (17, 58). In this study, we call these embryos *O-fut1*$^{R245A\ knock\text{-}in}$m/z.

O-fut1$^{R245A\ knock\text{-}in}$ *Homozygotes Obtained from Females Carrying the O-fut1*$^{R245A\ knock\text{-}in}$ *Homozygous Germ Line Show a Temperature-sensitive Neurogenic Phenotype*—In the embryonic central nervous system, the number of neuroblasts segregated from the neuroectoderm is determined by "lateral inhibition" through N signaling (59). A disruption of N signaling causes a failure of lateral inhibition, resulting in neuronal hyperplasia, known as the neurogenic phenotype (59). We studied the nervous system development in *O-fut1*$^{R245A\ knock\text{-}in}$m/z embryos at 25 and 30 °C, in case *O-fut1*^{R245A} had a temperature-sensitive property. Neurons were detected by anti-Elav antibody staining (Fig. 2, *A–J*). At 25 and 30 °C, the wild-type flies develop and reproduce normally, and their embryonic nervous system is also normal (Fig. 2, *A*, *B*, and *K*). In addition, the nervous system was normal in most of the *O-fut1*$^{R245A\ knock\text{-}in}$m/z embryos at 25 °C (Fig. 2, *C* and *K*; 1/38 embryos showed the neurogenic phenotype). However, at 30 °C, the *O-fut1*$^{R245A\ knock\text{-}in}$m/z embryos showed a highly penetrant neurogenic phenotype (Fig. 2, *D* and *K*, 15/15 embryos showed the neurogenic phenotype). This temperature-sensitive neurogenic phenotype has not been reported in previous studies using the transgenic *O-fut1*^{R245A} genomic locus (23, 24).

To confirm that the temperature-sensitive neurogenic phenotype was not due to the degradation of *O*-Fut1^{R245A} at 30 °C, we compared the protein levels of *O*-Fut1 and its derivative in wild-type and *O-fut1*$^{R245A\ knock\text{-}in}$ homozygous cells, respectively. We generated genetic mosaic wing discs composed of somatic clones homozygous for *O-fut1*^{4R6} or

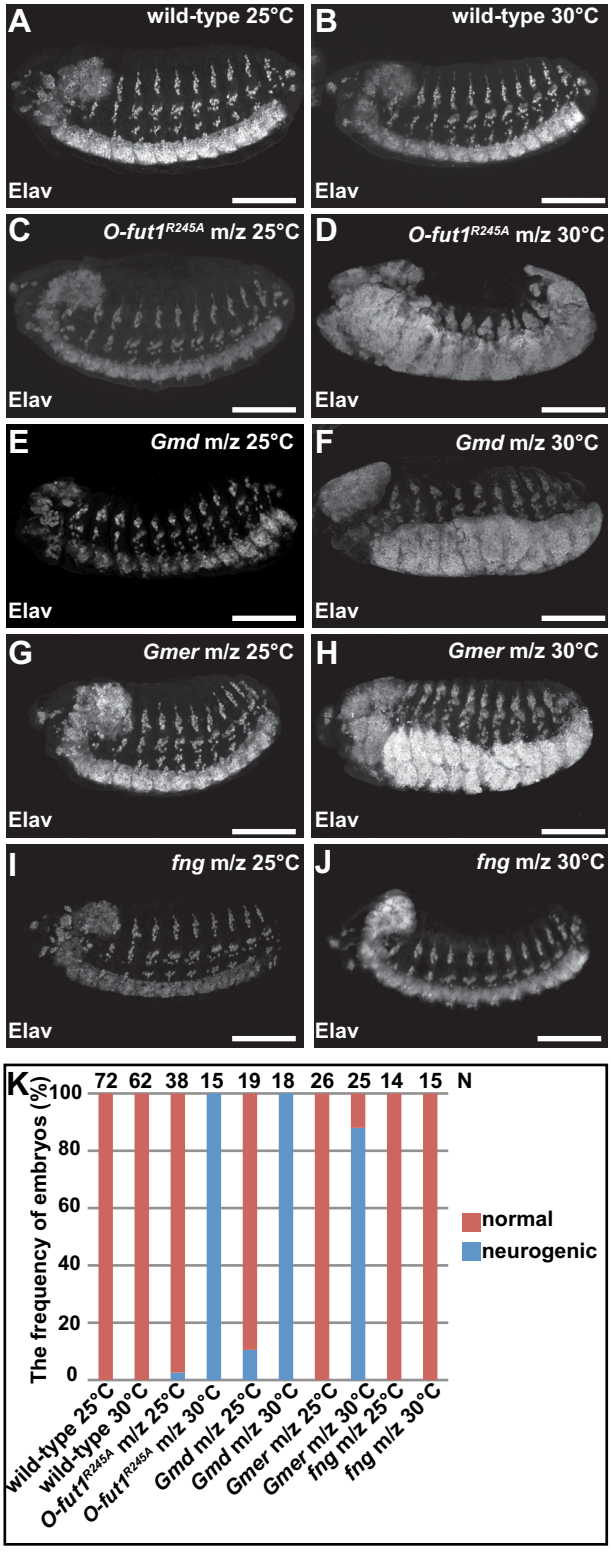

FIGURE 2. **Loss of *O*-fucose monosaccharide modification of N causes a neurogenic phenotype at 30 °C but not at 25 °C.** *A–J,* lateral views of embryos stained with an anti-Elav antibody (*white*). *A* and *B,* wild-type embryos raised at 25 °C (*A*) and 30 °C (*B*). *C* and *D, O-fut1*$^{R245A\ knock\text{-}in}$m/z raised at 25 °C (*C*) and 30 °C (*D*). *E* and *F, Gmd*^{H78}m/z raised at 25 °C (*E*) and 30 °C (*F*). *G* and *H, Gmer*^{SH}m/z raised at 25 °C (*G*) and 30 °C (*H*). *I* and *J, fng*^{13}m/z raised at 25 °C (*I*) and 30 °C (*J*). *K,* frequency of embryos (%) showing a normal central nervous system (*orange*) or a neurogenic phenotype (*blue*) at 25 and 30 °C. The number of embryos examined is shown at the top. *Scale bars,* 100 μm.

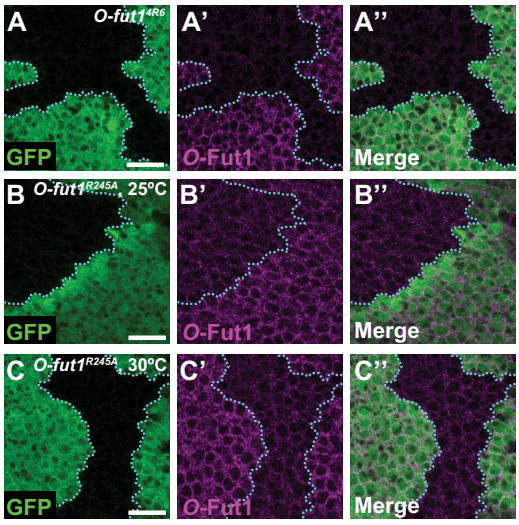

FIGURE 3. **O-Fut1 protein level in *O-fut1*$^{R245A\ knock\text{-}in}$ homozygous cells is the same at 25 and 30 °C.** *A–C″*, wing discs with *O-fut1*^{4R6} (*A–A″*) and *O-fut1*$^{R245A\ knock\text{-}in}$ (*B–C″*) mosaic clones, raised at 25 °C (*A–B″*) or 30 °C (*C–C‴*), were stained with an anti-*O*-Fut1 antibody (*magenta* in *A′*, *A″*, *B′*, *B″*, and *C′*, *C″*). Mosaic clones were identified by the absence of GFP (*green* in *A*, *A″*, *B*, *B″*, *C*, and *C″*). *A″*, *B″*, and *C″* show merged images of *A* and *A′*, *B and B′*, and *C* and *C′*, respectively. Boundaries of clones are indicated by *blue broken lines*. *Scale bars*, 10 μm.

O-fut1$^{R245A\ knock\text{-}in}$ and wild-type cells, and we detected the *O*-Fut1 proteins with an anti-*O*-Fut1 antibody (Fig. 3) (24). The intensity of immunostaining was greatly reduced in the *O-fut1*^{4R6} mutant cells, confirming the specificity of this antibody staining for the *O*-Fut1 protein, at 25 °C (Fig. 3, *A–A″*) (24). The level of the *O*-Fut1 protein derivative in the *O-fut1*$^{R245A\ knock\text{-}in}$ homozygous cells was slightly lower than that of the wild-type *O*-Fut1 protein in wild-type cells at 25 °C (Fig. 3, *B–B″*). However, no further reduction was observed at 30 °C (Fig. 3, *B–C″*), suggesting that the temperature-sensitive phenotype of *O-fut1*$^{R245A\ knock\text{-}in}$ was not caused by a decrease in *O*-Fut1 protein. Note that an anti-*O*-Fut1 antibody that can detect the endogenous *O*-Fut1 protein on Western blots was not available, so we were unable to confirm this conclusion by quantitative biochemical approaches.

A null mutation of *O-fut1*, *O-fut1*^{4R6}, is known to result in a neurogenic phenotype even at 25 °C (17). Therefore, the largely normal phenotype of the *O-fut1*$^{R245A\ knock\text{-}in}$m/z embryos at this temperature may be attributable to an enzyme activity-independent function of *O*-Fut1.

O-Fucose Monosaccharide on the EGF-like-repeats of N Has a Temperature-sensitive Role in N Signaling, Which Is Independent of Its Further GlcNAc Modification by Fng—There are two possible explanations for the temperature-sensitive property of the *O-fut1*$^{R245A\ knock\text{-}in}$ mutation. First, the monosaccharide *O*-fucose modification of N may function in a temperature-sensitive manner. Second, the activity of the *O-fut1*$^{R245A\ knock\text{-}in}$ gene and/or its product may be temperature-sensitive. To distinguish between these possibilities, we examined whether mutations of other genes that abolish the *O*-fucosylation of N also show a temperature-sensitive neurogenic phenotype.

Fucosylation requires GDP-fucose as the donor of fucose. In *Drosophila*, GDP-fucose is synthesized from GDP-mannose only through the *de novo* synthetic pathway (25, 32, 33, 60). GDP-mannose 4,6-dehydratase (Gmd) and GDP-4 keto-6 deoxy-D-mannose epimerase/reductase (Gmer) are essential enzymes for this pathway (61). Therefore, null mutations of these genes, such as *Gmd*^{H78}and *Gmer*^{SH}, abolish GDP-fucose synthesis in *Drosophila* (25, 33).

We observed embryos homozygous for *Gmd*^{H78} or *Gmer*^{SH} lacking their maternal contributions (*Gmd*^{H78}m/z and *Gmer*^{SH}m/z). We found that most of the *Gmd*^{H78}m/z (2/19 embryos showed the neurogenic phenotype) and *Gmer*^{SH}m/z (0/26 embryos showed the neurogenic phenotype) embryos had a normal nervous system at 25 °C (Fig. 2, *E*, *G*, and *K*). However, as found in the *O-fut1*$^{R245A\ knock\text{-}in}$m/z embryos, at 30 °C the neurogenic phenotype was highly penetrant in embryos with either the *Gmd*^{H78}m/z (18/18 neurogenic embryos) or the *Gmer*^{SH}m/z (23/25 neurogenic embryos) mutation (Fig. 2, *F*, *H*, and *K*). In these embryos, various fucose modifications, including the fucosylation of *N*-glycan, should be abolished. However, the collective results obtained from the *O-fut1*$^{R245A\ knock\text{-}in}$m/z, *Gmd*^{H78}m/z, and *Gmer*^{SH}m/z embryos indicated that the requirement for the monosaccharide *O*-fucose modification of N might be temperature-sensitive.

A contribution of *fng* to lateral inhibition has not been reported (22). However, to exclude the possibility that the temperature-sensitive neurogenic phenotype was caused by the lack of GlcNAc modification of *O*-fucose by Fng, we generated embryos homozygous for *fng*^{13} and lacking its maternal contribution (*fng*^{13}m/z). The *fng*^{13}m/z embryos did not show the neurogenic phenotype at either 25 °C ($n = 14$) or 30 °C ($n = 15$) in any case examined (Fig. 2, *I–K*). This finding indicated that the absence of GlcNAc modification by Fng is irrelevant to the temperature-sensitive neurogenic phenotype observed in the *O-fut1*$^{R245A\ knock\text{-}in}$m/z, *Gmd*^{H78}m/z, and *Gmer*^{SH}m/z embryos. Together, these findings indicate that the *O*-fucose monosaccharide modification of N is essential for N signaling during lateral inhibition at 30 °C but not at 25 °C.

O-Fucose Monosaccharide Modification of N Is Generally Required to Activate N Signaling at 30 °C—We next examined whether the *O*-fucose monosaccharide modification of N is generally required for N signaling at 30 °C. For this analysis, we generated somatic mosaic clones homozygous for *O-fut1*$^{R245A\ knock\text{-}in}$ in the wing discs of third-instar larvae, using the FLP/FRT system (Fig. 4, *B–C′*). The expression of *cut* along the D/V boundary of wild-type wing discs is induced by N signaling (Fig. 4*A*). In the mosaic wing discs, *cut* was also ectopically expressed along the boundaries of the *O-fut1*$^{R245A\ knock\text{-}in}$ somatic homozygous clones (marked by the absence of GFP) located in the dorsal compartment, at 25 °C (Fig. 4, *B* and *B′*). This phenotype was similar to that of somatic mosaic clones homozygous for *fng*^{13} (Fig. 4, *D–E′*) at 25 and 30 °C (62). Therefore, the absence of monosaccharide *O*-fucose had a similar defect in *cut* activation at 25 °C as did the absence of GlcNAc on *O*-fucose. This result is consistent with the previous conclusion that *O*-fucose monosaccharide does not have a specific function in N signaling at 25 °C (24). However, at 30 °C, the ectopic expression of *cut* along the boundaries of somatic mosaic clones homozygous for *O-fut1*$^{R245A\ knock\text{-}in}$ was abolished (Fig. 4, *C* and *C′*), supporting the idea that the monosaccharide form of *O*-fucose plays an essential role in N signaling in

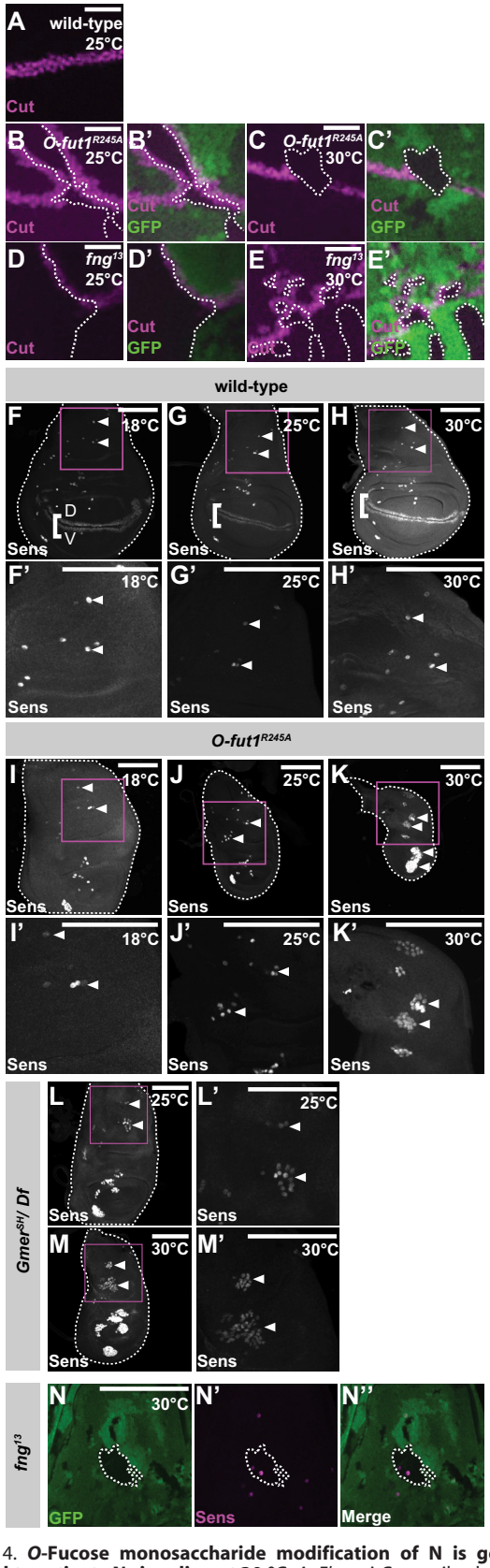

FIGURE 4. ***O*-Fucose monosaccharide modification of N is generally required to activate N signaling at 30 °C.** *A–E′*, anti-Cut antibody staining (*magenta*) of wing discs with wild-type (*A*), *O-fut1*$^{R245A\ knock\text{-}in}$ (*B–C′*), or *fng*^{13} (*D–E′*) mosaic clones. *B–E′*, mosaic clones were identified by the absence of GFP (*green*). Wing discs were isolated from larvae raised at 25 °C (*A, B, B′, D,* and *D′*) or 30 °C (*C, C′, E,* and *E′*). *B′*, *C′*, *D′*, and *E′* show merged images of GFP and Cut staining from *B* to *E*. Boundaries of mosaic clones are indicated by *broken lines*. *F–M′*, SOPs in wing discs were detected by anti-Sens antibody staining. *F–H′*, wild-type wing discs were isolated from larvae raised at 18 °C (*F* and *F′*), 25 °C (*G* and *G′*), or 30 °C (*H* and *H′*). Along the D/V boundary, the expression of *sens*, which is induced by *fng*-dependent N signaling, is shown by *white brackets* in *F–H*. *I–M′*, SOPs in wing discs of *O-fut1*$^{R245A\ knock\text{-}in}$ homozygotes (*I–K′*) and of heterozygotes between *Gmer*^{SH} and a deletion uncovering the *Gmer* locus (*Gmer*^{SH}*/Df*) (*L–M′*) are shown. Wing discs were isolated from larvae raised at 18 °C (*I* and *I′*), 25 °C (*J, J′, L,* and *L′*), or 30 °C (*K, K′, M,* and *M′*). *F′–M′* show magnified views of the *magenta squares* in *F–M*, respectively. *Arrowheads* indicate SOPs in *F–M′*. Wing discs are outlined by *broken lines*. *N–N″*, SOPs in wing discs with *fng*^{13} homozygote mosaic clones (detected by the absence of GFP, shown in *green*) were detected by anti-Sens antibody staining (*magenta*). Boundaries of mosaic clones are indicated by *broken lines*. Wing discs were isolated from larvae raised at 30 °C. *N″* shows merged images of *N* and *N′*. *Scale bars,* 20 μm for *A–E*, and 100 μm for *F–N*.

various developmental contexts at 30 °C. We also noted that the monosaccharide *O*-fucose was cell-autonomously required for the activation of N signaling at 30 °C (Fig. 4, *C* and *C′*), which is consistent with the idea that the *O*-fucose monosaccharide attached to N is essential for N′s activity at this temperature.

To obtain more evidence for this idea, we examined the formation of sensory organ precursors (SOPs) in the wing discs of third-instar larvae homozygous for *O-fut1*$^{R245A\ knock\text{-}in}$. A single SOP is selected from each proneural cluster in the wing disc, where SOPs arise in a well defined pattern at the third instar (63). In wild-type wing discs, the SOP formation pattern, observed by anti-Senseless (Sens) staining, was essentially the same from 18 to 30 °C (Fig. 4, *F–H′*). In the wing discs of *O-fut1*$^{R245A\ knock\text{-}in}$ homozygotes, SOPs did not form along the D/V boundary, because this SOP formation depends on the expression of *wg*, which is induced by the *fng*-dependent activation of N signaling (Fig. 4, *I–K*) (62). At 18 and 25 °C, the number of SOPs elsewhere in the wing discs increased slightly (Fig. 4, *I–J′*). However, these SOPs markedly increased in these wing discs at 30 °C (Fig. 4, *K* and *K′*). These results suggest that lateral inhibition was disrupted in the wing discs of *O-fut1*$^{R245A\ knock\text{-}in}$ homozygotes in a temperature-sensitive manner, as found in the embryonic central nervous system.

We also examined the SOP formation in the wing discs in the absence of *Gmer* function. A trans-heterozygote of *Gmer*^{SH} and a deletion mutant uncovering the *Gmer* locus survived until the third-instar larval stage, when we could isolate the wing discs to study SOP formation (33). At 25 °C, the number of SOPs increased slightly in these wing discs, although they did not form along the D/V boundary due to the absence of N signaling there (Fig. 4, *L* and *L′*). Nevertheless, the SOPs, except for those located at the D/V boundary, noticeably increased at 30 °C (Fig. 4, *M* and *M′*). We also confirmed that the SOP number was not affected in somatic mosaic clones homozygous for *fng*^{13} in the wing discs of third-instar larvae, even at 30 °C (Fig. 4, *N–N″*). Based on these results, we concluded that the monosaccharide form of *O*-fucose is generally required for N signaling at 30 °C, although we could not exclude the possibility that some exceptions exist.

O-Fucose Monosaccharide Modification of N Functions Upstream of the Membrane-tethered Form of Activated N at 30 °C—To assess the function of the *O*-fucose monosaccharide modification of N′s EGF-like repeats, we performed a set of

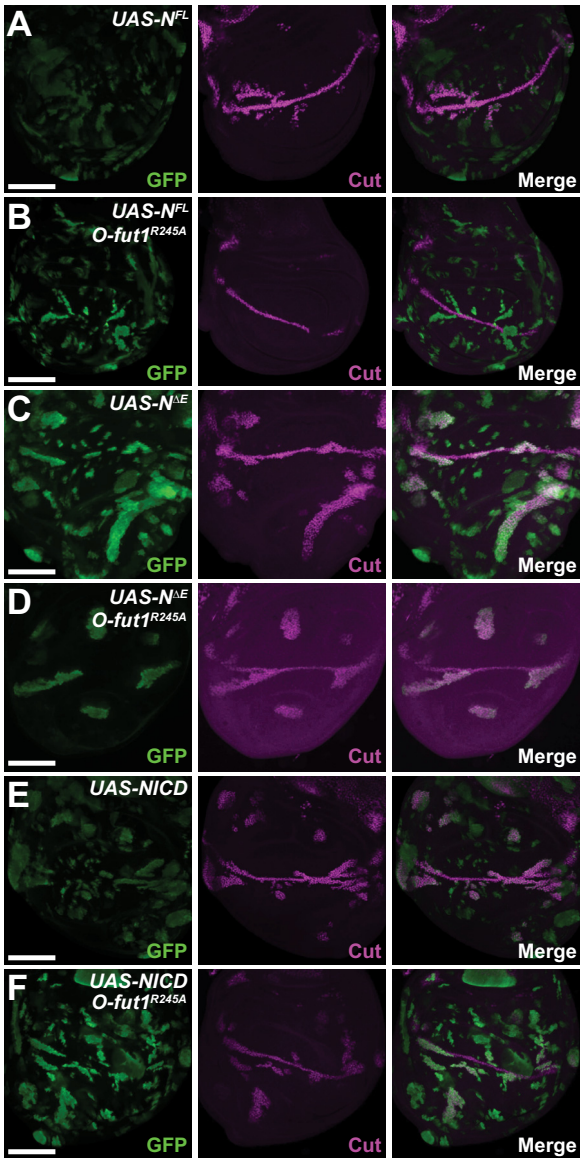

FIGURE 5. ***O*-Fucose monosaccharide modification of N functions upstream of the membrane-tethered form of activated N.** *A–F,* expression of *cut* in the wing discs of third-instar larvae was detected by anti-Cut antibody staining (*magenta* in *A–F*). *A* and *B,* mosaic clones overexpressing full-length N (N^{FL}) (*green* in *A* and *B*) in wild-type (*A*) or *O-fut1*$^{R245A\ knock\text{-}in}$ homozygote mosaic clones (*B*). *C* and *D,* mosaic clones overexpressing a membrane-tethered form of activated N ($N^{\Delta E}$) (*green* in *C* and *D*) in wild-type (*C*) or *O-fut1*$^{R245A\ knock\text{-}in}$ homozygote mosaic clones (*D*). *E* and *F,* mosaic clones overexpressing the intracellular domain of N (nuclear form of activated N) (*NICD*) (*green* in *E* and *F*) in wild-type (*E*) or *O-fut1*$^{R245A\ knock\text{-}in}$ homozygote mosaic clones (*F*). Wing discs were isolated from larvae cultured at 30 °C. *Scale bars,* 100 μm.

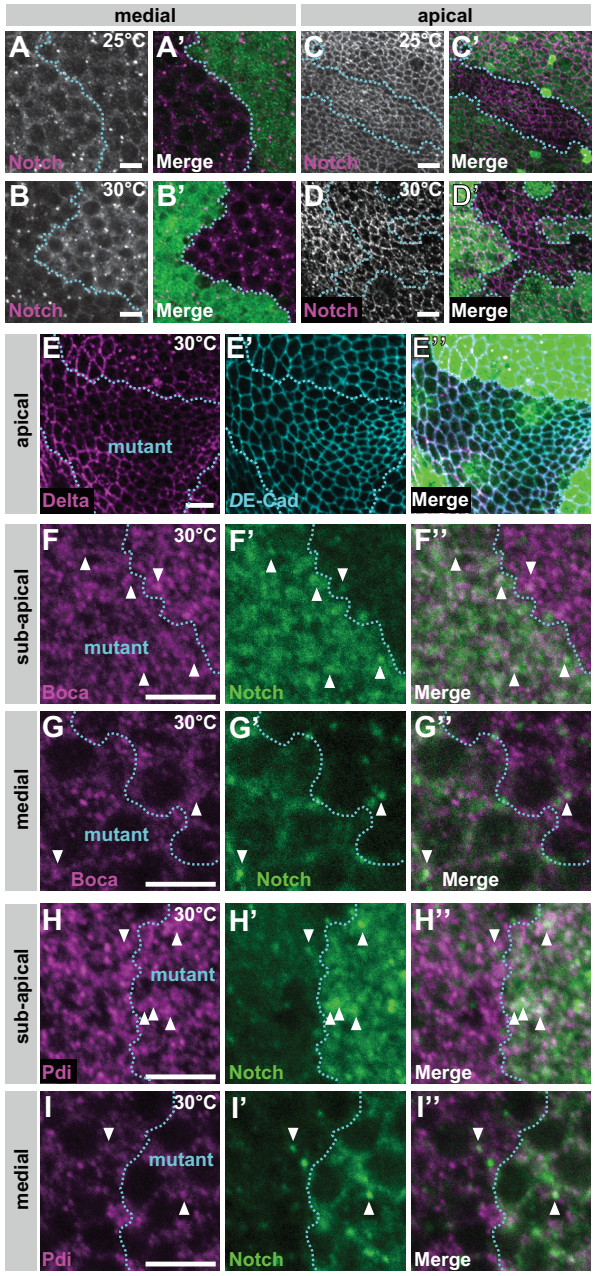

FIGURE 6. ***O*-Fucose monosaccharides on N are required for the proper localization of N at 30 °C.** *A–D′,* wing discs with mosaic clones homozygous for *O-fut1*$^{R245A\ knock\text{-}in}$, indicated by the absence of GFP (*A′*, *B′*, *C′*, and *D′*), were isolated from larvae raised at 25 °C (*A, A′, C,* and *C′*) or 30 °C (*B, B′, D,* and *D′*). Permeabilized (*A–B′*; medial plane) and nonpermeabilized (*C–D′*; apical plane) wing discs were stained with antibodies against N's intracellular and extracellular domains, respectively. Boundaries of clones are indicated by *broken blue lines*. *A′*, *B′*, *C′*, and *D′* show merged images of N and GFP staining in *A–D*. *E–I″*, Wing discs with mosaic clones homozygous for *O-fut1*$^{R245A\ knock\text{-}in}$; regions of mutants are outlined by *broken blue lines*. Wing discs isolated from larvae raised at 30 °C were permeabilized before antibody staining. *E–E″*, distributions of Delta (*magenta* in *E* and *E″*) and *DE*-Cad (*blue* in *E′* and *E″*) at the apical plane are shown. *E″* shows merged images of GFP, Delta (*E*), and *DE*-Cad staining (*E′*). *F–G″*, intracellular distributions of Boca (*magenta* in *F, F″, G,* and *G″*) and N (*green* in *F′*, *F″*, *G′*, and *G″*) were detected by immunostaining. *F–F″* and *G–G″* show optical sections of sub-apical and medial regions, respectively. *F″* and *G″* show merged images of *F* and *F′* and *G* and *G′*, respectively. *Arrowheads* indicate vesicles with N and Boca co-localization. *H–I″*, intracellular distributions of Pdi (*magenta* in *H, H″, I,* and *I″*) and N (*green* in *H′*, *H″*, *I′*, and *I″*) were detected by immunostaining. *H–H″* and *I–I″* show optical sections of the sub-apical and medial regions, respectively. *H″* and *I″* show merged images of *H* and *H′* and *I* and *I′*, respectively. *Arrowheads* indicate vesicles with N and Pdi co-localization. *Scale bars,* 5 μm.

epistasis analyses involving *O-fut1*$^{R245A\ knock\text{-}in}$ and various derivatives of *N*. We used the MARCM system (43) to produce full-length N (N^{FL}), a membrane-tethered form of activated N ($N^{\Delta E}$), and the N intracellular domain (NICD) in somatic mosaic clones homozygous for *O-fut1*$^{R245A\ knock\text{-}in}$ at 30 °C (Fig. 5). In wild-type wing discs, the overexpression of N^{FL}, $N^{\Delta E}$, or *NICD* resulted in the ectopic induction of *cut* at 30 °C (Fig. 5, *A, C,* and *E*). However, the overexpression of N^{FL} failed to induce ectopic *cut* expression in the somatic clones homozygous for *O-fut1*$^{R245A\ knock\text{-}in}$ at 30 °C (Fig. 5*B*). Thus, *O-fut1*$^{R245A\ knock\text{-}in}$ was epistatic to N^{FL} under this condition. By contrast, the

TABLE 1

Quantitative analysis of co-localization between N protein and various markers of intracellular compartments in *O-fut1*$^{R245A\ knock\text{-}in}$ or *O-fut1*^{4R6} mutant cells, or *O-fut1*$^{R245A\ knock\text{-}in}$ and *rumi* double-mutant cells

Somatic mosaic clones homozygous or double homozygous for the indicated mutants were induced in wing discs of larvae cultured at 25 or 30 °C, as indicated. Control cells heterozygous for *O-fut1*$^{R245A\ knock\text{-}in}$ were in the wing discs with somatic mosaic clones of *O-fut1*$^{R245A\ knock\text{-}in}$ homozygotes. The percentage of vesicles positive for each marker that were also positive for N is shown. The ER was detected with two markers, Boca and Pdi, at two different optical planes, sub-apical (SA) and medial. The ER showed an indistinct and shapeless structure at the sub-apical plane. N protein distribution with Boca or Pdi is indicated by + (co-localizing) or − (not co-localizing). The MARCM system was used to express *UAS-Lamp-HRP*. All the N-positive vesicles and vesicles positive for each marker were counted in 32 × 32-μm square areas of representative Z-series confocal images. Three to six independent images were analyzed for each experiment. Asterisks show statistically significant results ($p < 0.05$), compared with control. Standard errors are shown, following ± symbol. ND means not determined.

		control at 25°C	control at 30°C	*O-fut1*^{R245A} at 25°C	*O-fut1*^{R245A} at 30°C	*O-fut1*^{4R6} at 25°C	*O-fut1*^{4R6} at 30°C	*rumi*^{44} at 25°C	*O-fut1*^{R245A} *rumi*^{44} at 25°C
ER (Boca)	SA	-	-	-	+	+	+	-	+
	medial	0.79±0.28	1.2±0.12	0.88±0.30	1.2±0.11	1.2±0.11	1.5±0.33	1.3±0.11	1.1±0.10
ER (Pdi)	SA	-	-	-	+	+	+	-	+
	medial	1.3±0.055	2.0±0.44	1.5±0.078	2.1±0.14	1.2±0.21	2.4±0.27	1.4±0.17	1.8±0.48
Golgi (GM130)		1.2±0.11	0.87±0.10	1.2±0.087	1.2±0.32	0.58±0.17	1.2±0.40	1.7±0.25	1.2±0.15
early endosome (Hrs)		6.7±1.9	13±2.4	8.9±1.7	23±2.8*	8.1±0.71	9.6±0.94	7.0±0.85	7.8±0.87
late endosome (Rab7)		6.7±1.5	7.2±0.68	6.8±1.6	8.1±1.4	3.5±1.3	5.0±0.92	6.0±0.56	4.7±0.62
recycling endosome (Rab11)		0.79±0.28	0.86±0.26	0.88±0.30	1.6±0.61	0.76±0.11	0.99±0.26	0.80±0.17	0.64±0.061
lysosome (Lamp-HRP)		5.0±1.4	6.9±2.1	8.0±1.1	21±3.4*	11±2.4	11±2.6	ND	ND

overexpression of $N^{\Delta E}$ or *NICD* still induced the ectopic expression of *cut* in somatic mosaic clones homozygous for *O-fut1*$^{R245A\ knock\text{-}in}$ at 30 °C (Fig. 5, *D* and *F*). Therefore, the two activated forms of *N*, $N^{\Delta E}$ and *NICD*, were epistatic to *O-fut1*$^{R245A\ knock\text{-}in}$ under this condition. Based on these epistasis analyses, we speculated that the monosaccharide *O*-fucose modification of N is required downstream of full-length N and upstream of the S3 cleavages of N.

O-Fucose Monosaccharide Modification of N Is Required for the Proper Localization of N at 30 °C—To understand how the monosaccharide *O*-fucose modification of N affects N signaling, we compared N′s subcellular localization at 25 and at 30 °C in somatic mosaic clones homozygous for *O-fut1*$^{R245A\ knock\text{-}in}$ in the wing discs of third-instar larvae (Fig. 6). In epithelial cells in wild-type wing discs, most of the N protein is detected in the sub-apical region and the adherence junctions at 25 °C, although it is also detected in intracellular vesicles (26, 64).

To detect total cellular N protein, we stained permeabilized wing discs with an antibody against N′s intracellular domain (Fig. 6, *A*–*B*′), which showed N distribution at the optical plane corresponding to the middle of the epithelial cells at 25 °C (Fig. 6, *A* and *A*′) and 30 °C (Fig. 6, *B* and *B*′). At 25 °C, there were no marked abnormalities in the intracellular N distribution in somatic mosaic clones homozygous for *O-fut1*$^{R245A\ knock\text{-}in}$ (Fig. 6, *A* and *A*′); however, at 30 °C, N accumulated inside the cell (Fig. 6, *B* and *B*′) although other membrane proteins, such as Dl and *D*E-cadherin (*D*E-Cad), were distributed normally under the same conditions (Fig. 6, *E*–*E*″).

To visualize N protein delivered to the epithelial cell surface at the sub-apical region, nonpermeabilized wing discs carrying

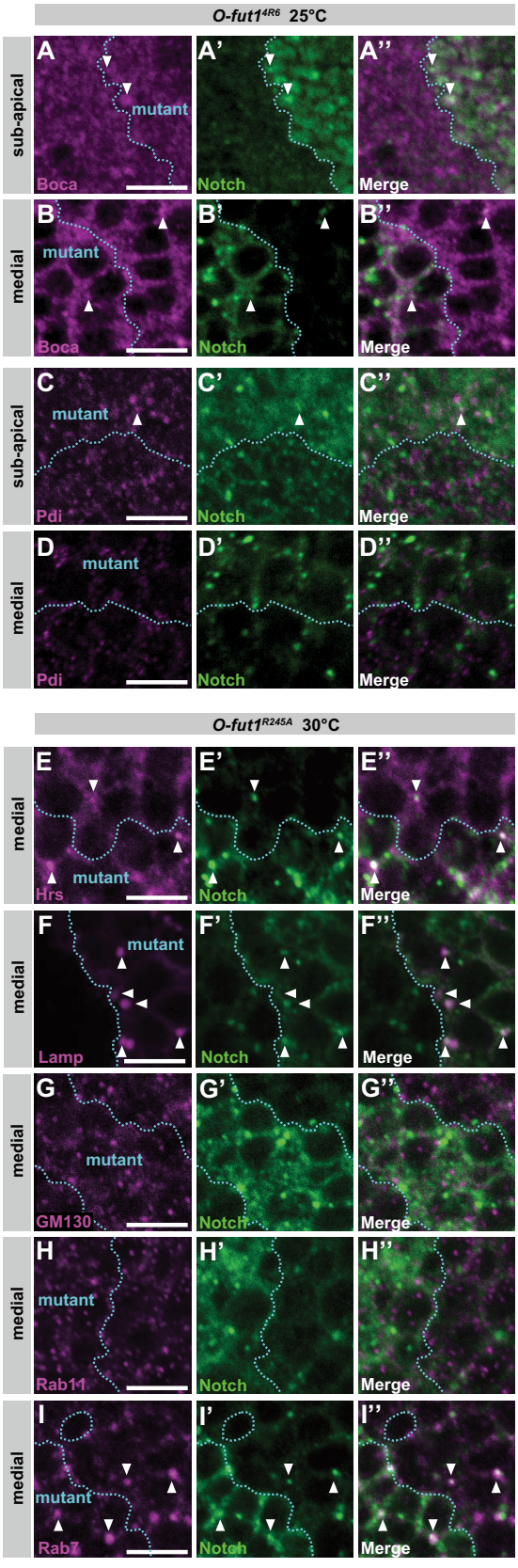

FIGURE 7. **Co-localization of intracellular vesicular compartment markers with N in *O-fut1*^{R245A} somatic mosaic clones.** *A–D″*, wing discs with *O-fut1*^{4R6} homozygote mosaic clones. Regions of mutants outlined by *broken blue lines* were double-stained with an anti-Boca (*magenta* in *A*, *A″*, *B*, and *B″*) or anti-Pdi (*C*, *C″*, *D*, and *D″*) antibody and an anti-N antibody (*green* in *A′*, *A″*, *B′*, *B″*, *C′*, *C″*, *D′*, and *D″*). Wing discs were isolated from larvae raised at 25 °C. somatic mosaic clones homozygous for *O-fut1*$^{R245A\ knock\text{-}in}$ were stained with an antibody against the extracellular domain of N (Fig. 6, *C–D′*) (65). The amount of cell-surface N at the sub-apical plane was the same at 25 or 30 °C in cells homozygous for *O-fut1*$^{R245A\ knock\text{-}in}$ under this condition (Fig. 6, *C–D′*). Thus, even at 30 °C, N delivery to the cell surface was not disrupted in cells homozygous for *O-fut1*$^{R245A\ knock\text{-}in}$, although N accumulated within these cells (Fig. 6, *B* and *B′*). However, intracellular and cell-surface N protein did not accumulate in somatic mosaic clones homozygous for *fng*^{13} at 25 or 30 °C, suggesting that the intracellular accumulation of N could not be attributed to the GlcNAc modification of *O*-fucose (data not shown).

We next determined the intracellular compartments in which N accumulated in the somatic mosaic clones homozygous for *O-fut1*$^{R245A\ knock\text{-}in}$ at 30 °C. We identified the ER (Boca and Pdi), Golgi (GM130), early endosomes (Hrs), late endosomes (Rab7), recycling endosomes (Rab11), and lysosomes (Lamp) by immunostaining (25, 36, 51, 52, 54). In wing-disc epithelial cells, the ER was detected either as an indistinct and shapeless structure (Fig. 6, *F–F″* and *H–H″*) or as dots (Fig. 6, *G–G″* and *I–I″*). The former was detected mostly in the cells' apical regions (Fig. 6, *F–F″* and *H–H″*), and the latter in more basal regions (Fig. 6, *G–G″* and *I–I″*). These structures were recognized by antibodies against two ER-marker proteins, Boca (Fig. 6, *F–G″*) and Pdi (Fig. 6, *H–I″*). To analyze the co-localization of N and markers for various intracellular compartments quantitatively, the percentage of vesicles positive for each marker that was also positive for N is shown in Table 1. At 30 °C, the distribution of accumulated N protein overlapped partly with the indistinct and shapeless ER in somatic mosaic clones homozygous for *O-fut1*$^{R245A\ knock\text{-}in}$ (*white arrowhead* in Fig. 6, *F–F″*, and *H–H″*, and Table 1), although hardly any N protein was detected in this structure in *O-fut1*$^{R245A\ knock\text{-}in}$/+ (control) cells (Fig. 6, *F–F″*, and *H–H″*, and Table 1). However, there was no increase in N-protein level in the dot-structure ER in the cells homozygous for *O-fut1*$^{R245A\ knock\text{-}in}$, compared with this ER in *O-fut1*$^{R245A\ knock\text{-}in}$/+ cells at 30 °C (*white arrowheads* in Fig. 6, *G–G″*, and *I–I″*, and Table 1). Therefore, N accumulation in the indistinct and shapeless ER structures but

Optical sections of sub-apical (*A–A″* and *C–C″*) and medial regions (*B–B″* and *D–D″*) are shown. *A″–D″* show merged images from *A–D* and *A′–D′*, respectively. *E–I″*, wing discs with mosaic clones homozygous for *O-fut1*$^{R245A\ knock\text{-}in}$; regions of mutants are outlined by *broken blue lines*. Wing discs isolated from larvae raised at 30 °C were permeabilized before antibody staining. *E–E″*, intracellular distributions of Hrs (*magenta* in *E* and *E″*) and N (*green* in *E′* and *E″*) were detected by immunostaining at the medial plane. *E″* shows merged images from *E* and *E′*. *Arrowheads* indicate vesicles with N and Hrs co-localization. *F–F″*, using the MARCM system, *UAS-Lamp-HRP* was overexpressed in mosaic clones homozygous for *O-fut1*$^{R245A\ knock\text{-}in}$, which were detected by the presence of Lamp-HRP protein (*magenta* in *F* and *F″*). The intracellular distribution of N was detected by immunostaining (*green* in *F′* and *F″*). *F″* shows merged images from *F* and *F′*. *Arrowheads* indicate vesicles with N and Lamp-HRP co-localization. *G–G″*, intracellular distributions of GM130 (*magenta* in *G* and *G″*) and N (*green* in *G′* and *G″*) were detected by immunostaining at the medial plane. *G″* shows merged images from *G* and *G′*. *H–H″*, intracellular distributions of Rab11 (*magenta* in *H* and *H″*) and N (*green* in *H′* and *H″*) were detected by immunostaining at the medial plane. *H″* shows merged images from *H* and *H′*. *I–I″*, intracellular distributions of Rab7 (*magenta* in *I* and *I″*) and N (*green* in *I′* and *I″*) were detected by immunostaining at the medial plane. *I″* shows merged images from *I* and *I′*. *Arrowheads* indicate vesicles where N co-localized with rab7. *Scale bars*, 5 μm.

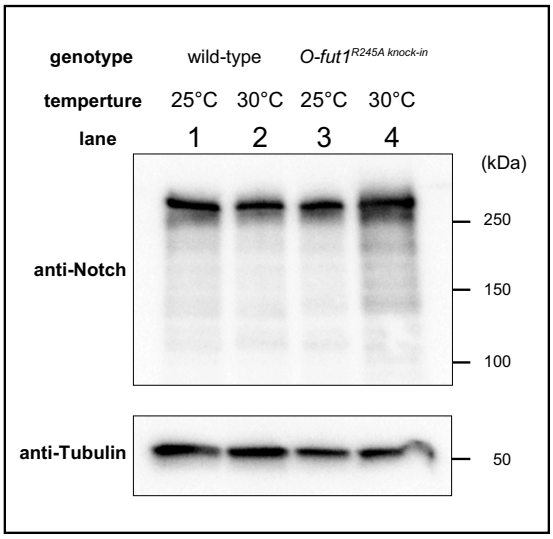

FIGURE 8. **Amount and size of N protein detected by Western blot are not altered in *O-fut1*$^{R245A\ knock\text{-}in}$ homozygote wing imaginal discs.** N protein was detected by Western blot using an anti-N antibody (C17.9C6) (*upper panel*). Protein extracts were prepared from wing discs isolated from third-instar larvae. *Lane 1*, wild-type cultured at 25 °C; *lane 2*, wild-type cultured at 30 °C; *lane 3*, *O-fut1*$^{R245A\ knock\text{-}in}$ homozygote cultured at 25 °C; *lane 4*, *O-fut1*$^{R245A\ knock\text{-}in}$ homozygote cultured at 30 °C. As a loading control, α-tubulin was detected (*lower panel*). Positions of molecular mass markers are shown at right (*kDa*).

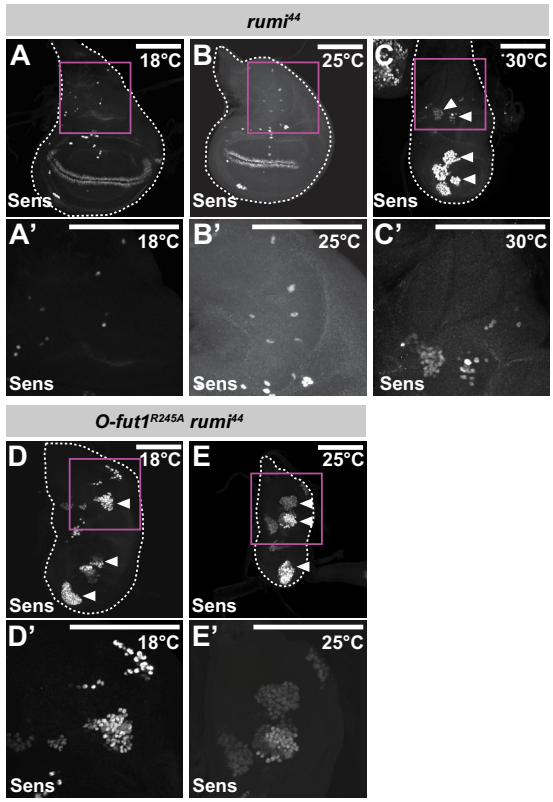

FIGURE 9. ***O*-Fucose and *O*-glucose modifications of N function redundantly in the activation of N signaling.** *A–E′*, SOPs in wing discs were detected by anti-Sens antibody staining. SOPs in *rumi*^{44} homozygote wing discs were isolated from larvae raised at 18 °C (*A* and *A′*), 25 °C (*B* and *B′*), or 30 °C (*C* and *C′*). SOPs in wing discs homozygous for *O-fut1*$^{R245A\ knock\text{-}in}$ and *rumi*^{44} were isolated from larvae raised at 18 °C (*D* and *D′*) or 25 °C (*E* and *E′*). *Arrowheads* indicate hyperplastic SOPs. Outlines of wing discs are shown by *broken lines*. *A′–E′* show magnified views of the areas in *magenta squares* in *A–E*, respectively. *Scale bars,* 100 μm.

not the dot-shaped ER structures may coincide with the loss of N signaling activity.

Although N is reported to accumulate in the ER in somatic clones homozygous for *O-fut1*^{4R6}, a null mutant of *O-fut1* (17), there are conflicting reports (23, 25). Here, we found that accumulated N partially overlapped with indistinct, shapeless ER structures, although there was no change of the amount of N in dot-shaped ER at 25 or 30 °C (Fig. 7, *A–D‴*, and Table 1). This may account for the previous discrepancy in the ER accumulation of N reported in *O-fut1*^{4R6} mutant cells. Nonpermeabilized staining did not detect N protein at the sub-apical cell-surface region in *O-fut1*^{4R6} mutant epithelial cells at 25 or 30 °C; this agreed with previously reported findings at 25 °C (data not shown) (23, 25).

We also observed that N protein was detected more often in early endosomes (23 ± 2.8) and lysosomes (21 ± 3.4) in somatic mosaic clones homozygous for *O-fut1*$^{R245A\ knock\text{-}in}$ at 30 °C, compared with those at 25 °C or with control cells (13 ± 2.4 and 4.4 ± 0.59, respectively) (Fig. 7, *E–F″* and Table 1). These differences were statistically significant (*t* test, $p < 0.05$). In contrast, there was no marked difference in N distribution in the Golgi, late endosomes, or recycling endosomes of these cells at either temperature (Fig. 7, *G–I″* and Table 1). These data suggest that the *O*-fucose monosaccharide modification of N may be required for specific step(s) of N′s trafficking at 30 °C but not at 25 °C. In addition, the distinct defects in N′s trafficking found in *O-fut1*$^{R245A\ knock\text{-}in}$ mutant cells *versus* *O-fut1*^{4R6} mutant cells suggest that the nature of the defect in these two mutants is different (Table 1). These observations further support our idea that the temperature-sensitive phenotype of *O-fut1*$^{R245A\ knock\text{-}in}$ is not due to a temperature-dependent loss of *O-fut1* activity, associated with, for example, the breakdown of the *O*-Fut1^{R245A} mutant protein (Fig. 3). To detect possible alterations in the N protein in the *O-fut1*$^{R245A\ knock\text{-}in}$ mutant, including changes in its stability and processing, we detected the N protein in *O-fut1*$^{R245A\ knock\text{-}in}$ homozygous wing discs from the third-instar larvae cultured at 25 and 30 °C, by Western blot (Fig. 8). However, we did not observe any marked differences in the amount or size of the N protein between the mutant and the wild-type wing discs (compare *lanes 1* and *2* and *lanes 3* and *4* in Fig. 8).

O-Fucose and O-Glucose Modifications of N Function Redundantly—The EGF-like repeats of N have consensus sequences not only for *O*-fucose but also for *O*-glucose modifications (27). *O*-Glucose is added by Rumi, a protein *O*-glucosyltransferase in *Drosophila* (27, 28). In the absence of *rumi* function, temperature-sensitive phenotypes associated with the loss of N signaling, which are similar to those of *O-fut1*$^{R245A\ knock\text{-}in}$, are observed (27, 28). In somatic mosaic clones homozygous for *rumi*^{44}, a null mutation, N accumulated intracellularly, which was also reminiscent of a defect in *O-fut1*$^{R245A\ knock\text{-}in}$ homozygous cells. Therefore, we thought that the *O*-fucose monosaccharide modification of N might function redundantly with the *O*-glucose glycan modification of N in N signaling. To test this possibility, we generated a *rumi* and *O-fut1*$^{R245A\ knock\text{-}in}$ double mutant and observed SOP formation in the wing discs of third-instar larvae. As described

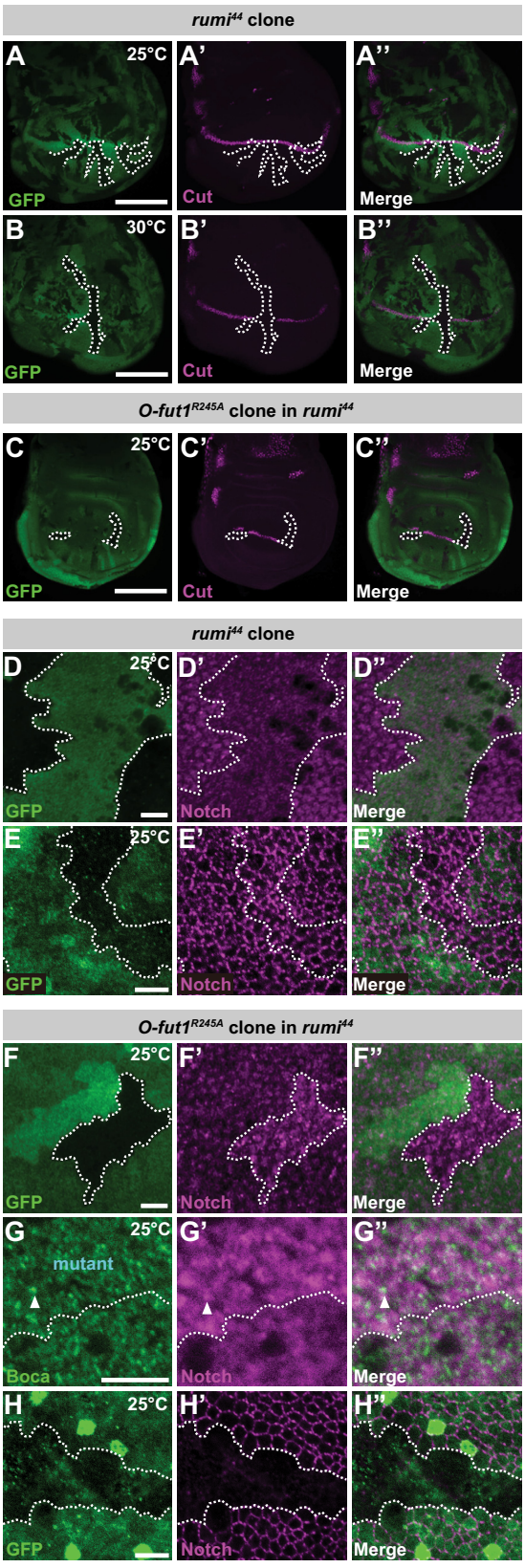

FIGURE 10. **Monosaccharide *O*-fucose and *O*-glucose glycan of N function redundantly in N signaling.** *A–B″*, anti-Cut antibody staining (*magenta*) of third-instar wing discs with mosaic clones homozygous for *rumi*^{44} (indicated by the absence of GFP, shown in *green*). The wing discs were isolated from larvae raised at 25 °C (*A–A″*) or 30 °C (*B–B″*). *C–C″*, anti-Cut antibody staining (*magenta*) of third-instar wing discs homozygous for *rumi*^{44} with mosaic clones homozygous for *O-fut1*$^{R245A\ knock\text{-}in}$ (indicated by the absence of GFP, shown in *green*). The wing discs were isolated from larvae raised at 25 °C. The boundaries of mosaic clones are indicated by *broken white lines*. *A″*, *B″*, and *C″* show merged images of *A*, *B*, and *C* and *A′*, *B′*, and *C′*, respectively. *D–H″*, permeabilized (*D–D″* and *F–G″*) or nonpermeabilized (*E–E″* and *H–H″*) wing discs were stained with antibodies against N's intracellular (*D–D″* and *F–G″*) or extracellular domains (*E–E″* and *H–H‴*). *D–E″*, wing discs with mosaic clones homozygous for *rumi*^{44} (indicated by the absence of GFP, shown in *green*). *F–H″*, wing discs of a *rumi*^{44} homozygote with mosaic clones homozygous for *O-fut1*$^{R245A\ knock\text{-}in}$ (indicated by the absence of GFP, shown in *green* in *F*, *F″*, *H*, and *H″* or labeled "mutant" in *G*). Borders of mosaic clones are indicated by *broken white lines*. *Scale bars*, 100 μm for *A–C″* and 5 μm for *D–H″*.

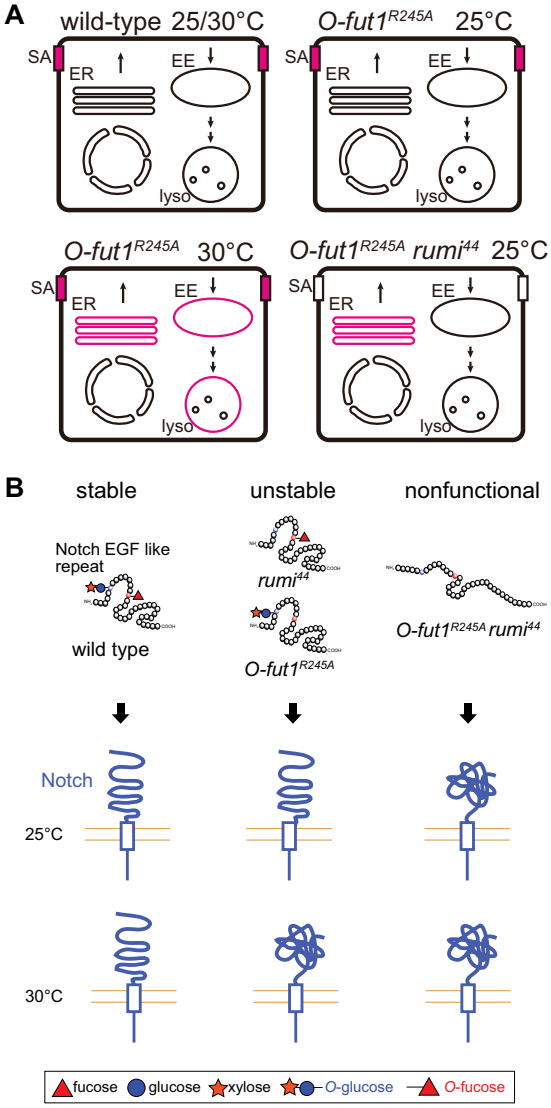

FIGURE 11. **Model of *O*-fucose and *O*-glucose on N and N accumulation in various mutants.** *A*, schematic diagram showing the intracellular compartment, in which N (*magenta*) is strongly accumulated in wild-type and various mutant cells. *EE*, early endosome; *lyso*, lysosome; *SA*, sub-apical region. *B*, schematic model of the redundant roles of *O*-fucose monosaccharide and *O*-glucose glycan modifications of the EGF-like repeats of N in the proper folding of the EGF-like repeats (*upper*), which may affect the entire extracellular structure of the full-length N (*lower*).

above, the number of SOPs increased at 30 °C in wing discs homozygous for *rumi*^{44}, but it was normal at 18 and 25 °C (Fig. 9, *A–C′*). This phenotype is very similar to that of *O-fut1*$^{R245A\ knock\text{-}in}$ wing discs (Fig. 4, *I–K′*). However, the number of SOPs increased in the wing discs homozygous for *rumi*^{44} and *O-fut1*$^{R245A\ knock\text{-}in}$ even at 18 and 25 °C, suggesting that N

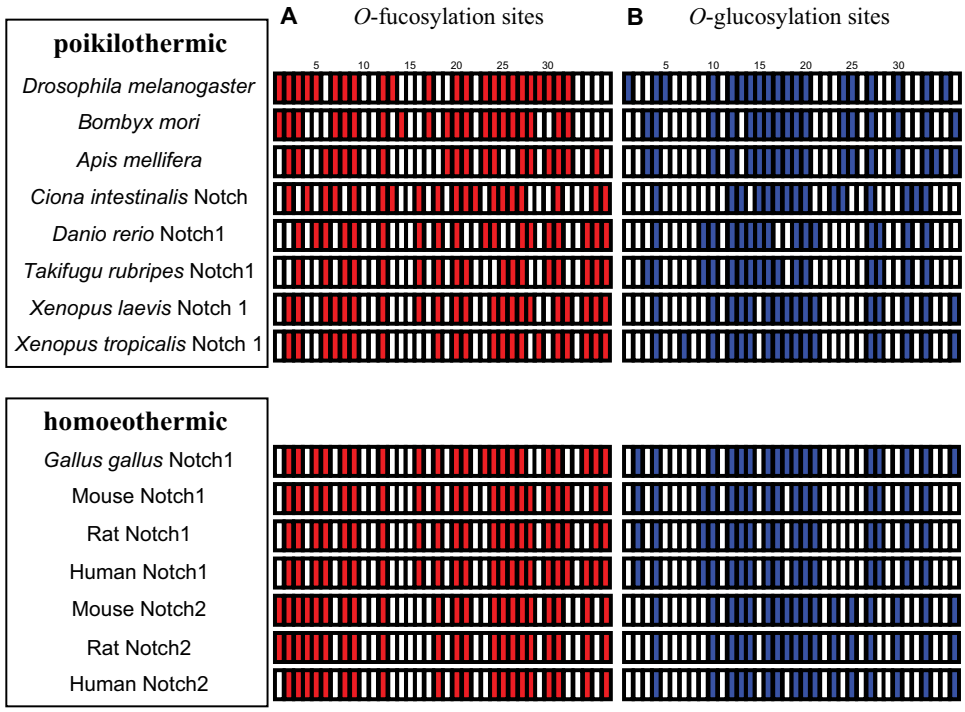

FIGURE 12. **Predicted *O*-fucosylation and *O*-glucosylation sites in the EGF-like repeats of various N receptors.** *A, red bars* show predicted *O*-fucosylation sites in the EGF-like repeats of various N proteins. *B, blue bars* show predicted *O*-glucosylation sites in the EGF-like repeats of various N proteins. The N proteins of poikilothermic and homoeothermic animals are grouped in the *upper* and *lower boxes*, respectively. Species are indicated at *left*.

signaling was abolished under these conditions (Fig. 9, *D–E′*). These results suggest that the *O*-fucose monosaccharide and *O*-glucose glycans have a redundant function during lateral inhibition that controls the number of SOPs in the wing discs.

Similar redundancy in the function of the *O*-fucose monosaccharide and *O*-glucose glycans was observed in the activation of N signaling along the D/V boundary of the wing disc at the third instar. The expression of *cut* along the D/V boundary disappeared at 30 °C in somatic mosaic clones homozygous for $rumi^{44}$ (Fig. 10, *B–B″*), but *cut*'s expression was normal at 25 °C (Fig. 10, *A–A″*). The phenotype of the somatic mosaic clones homozygous for $rumi^{44}$ at 30 °C was very similar to that of the somatic mosaic clones homozygous for $O\text{-}fut1^{R245A\ knock\text{-}in}$ at 30 °C (Fig. 4, *C* and *C′*). However, in somatic mosaic clones homozygous for $rumi^{44}$ and $O\text{-}fut1^{R245A\ knock\text{-}in}$, *cut* expression was abolished even at 25 °C (Fig. 10, *C–C″*).

The *O*-fucose monosaccharide and *O*-glucose glycans on the EGF-like repeats of N also collaborated to increase the amount of N at the sub-apical plasma membrane. As reported previously, slight accumulations of N protein were found in cells homozygous for $rumi^{44}$ alone, at 25 °C (Fig. 10, *D–D″*), although the amount of cell-surface N at the sub-apical region, detected by nonpermeabilized staining, was not altered in these cells (Fig. 10, *E–E″*) (27). However, the N-protein accumulations were more prominent in intracellular compartments in somatic mosaic clones homozygous for $rumi^{44}$ and $O\text{-}fut1^{R245A\ knock\text{-}in}$ (Fig. 10, *F–F″*). In these double mutant cells, the accumulated N partially co-localized with ER markers (Fig. 10, *G–G″*, and Table 1). Curiously, nonpermeabilized staining for N revealed that the cell-surface N was diminished in these cells (Fig. 10, *H–H″*), but it was unaffected in cells homozygous for either $O\text{-}fut1^{R245A\ knock\text{-}in}$ (Fig. 6, *C–D′*) or $rumi^{44}$ (Fig. 10, *E–E″*) (27). Therefore, *O*-fucose monosaccharide and *O*-glucose glycans have redundant roles, and in their absence N was not delivered to or stably maintained at the plasma membrane.

DISCUSSION

The functions of the monosaccharide *O*-fucose on the EGF-like repeats of N have been vague. In *Drosophila*, the monosaccharide *O*-fucose was proposed to serve primarily as an acceptor for Fng, with *O*-Fut1 being required as a specific chaperon for N (23, 24). However, in mammalian cells, the *O*-fucose modification was reported to be required for the optimal activation of N signaling under certain conditions (55). More recently, Fng-independent functions of fucosylation in *Drosophila* N signaling were reported, although these effects are relatively mild or cell type-specific (66, 67). In this study, we revealed that the *O*-fucose monosaccharide, independent of GlcNAc modification by Fng, is essential for N signaling at 30 °C in various developmental contexts in *Drosophila*. Moreover, in the absence of modifications with both *O*-fucose monosaccharide and *O*-glucose glycan, N signaling was abolished even at 25 °C, although the loss of either modification alone caused this phenotype only at 29–30 °C (27). The loss of N signaling coincides with a severe reduction of N at the sub-apical plasma membrane and an accumulation of N in a particular fraction of the ER (Figs. 10, *F–G″* and 11*A*). These results suggest that *O*-fucose monosaccharide and *O*-glucose glycan modifications of N have redundant and collaborative roles in the activation of N signaling and the proper localization of N at the sub-apical plasma membrane (Fig. 11*A*). However, at this point we could not distinguish between whether N failed to reach the plasma membrane or it failed to be stably maintained on the membrane under this double mutant condition.

The biochemical roles of the *O*-fucose monosaccharide and *O*-glucose glycan modifications are still elusive. However, a previous NMR study revealed that the fucose moiety directly functions as a "bridge" in the formation of an antiparallel β-sheet in EGF-like repeat 12 of mouse Notch1, stabilizing its structure through an interaction between the fucose and the peptide backbone of the EGF-like repeat (68). Therefore, we speculate that structural destabilization of each EGF-like repeat may affect the folding of the full-length N (Fig. 11*B*). Deficient N folding may explain our observation that N accumulated in the ER of cells homozygous for *O-fut1*$^{R245A\ knock\text{-}in}$ at 30 °C (Fig. 11*B*). More severe folding defects may occur in the absence of both *O*-fucose monosaccharide and *O*-glucose glycan modifications (Fig. 11*B*). It was previously shown that *O*-Fut1 and Rumi may be involved in quality control of the N protein, because they both only modify properly folded EGF-like repeats (69–71). Therefore, it is possible that full-length N with EGF-like repeats lacking *O*-fucose monosaccharide and *O*-glucose glycan modifications may escape from its chaperon, leading to misfolding of the full-length N. However, at this point, the mechanism by which the potential destabilization of EGF-like repeats influences the global structure of full-length N is unknown. Moreover, it was previously shown that disrupting the *O*-fucosylation site in the 12th EGF-like repeat of mouse Notch1 does not affect the amount of cell-surface Notch1, but instead it reduces Notch1's activation, suggesting that the *O*-fucose modification of the 12th EGF-like repeat does not play a role in Notch1's folding (72). Therefore, it is possible that the *O*-fucose modification on other EGF-like repeats is required for the folding of full-length N and that the *O*-fucose modification of N has multiple functions in N signaling.

Considering that the *O*-fucose monosaccharide and *O*-glucose glycan modifications of the EGF-like repeats may function to increase the heat stability of full-length N, it is tempting to speculate that some sites for these modifications are specifically conserved in animals with higher body temperatures (homeothermic) but not in those with lower temperatures (poikilothermic). However, a comparison of the consensus sequences for these modifications failed to find a correlation between body temperature and the evolutionary conservation of these sites (Fig. 12).

A number of protein motifs contain multiple glycosylation sites for different types of glycan modifications (73). In this study, we found that the *O*-fucose monosaccharide and *O*-glucose glycan modifications of the EGF-like repeats of N have a redundant role, possibly in the folding of N. Thus, our results provide a case in which different types of glycosylation occurring at a protein motif may play a common and collaborative role.

Acknowledgments—We thank Hamed Jafer-Nejad, Jürgen Knoblich, David Bilder, the Bloomington Stock Center, and the Drosophila Genetic Resource Center for flies and Hugo Bellen, Kenneth D. Irvine, Richard S. Mann, Akira Nakamura, and the Developmental Studies Hybridoma Bank for antibodies.

REFERENCES

1. Artavanis-Tsakonas, S., Rand, M. D., and Lake, R. J. (1999) Notch signaling: cell fate control and signal integration in development. *Science* **284,** 770–776
2. Bray, S. J. (2006) Notch signalling: a simple pathway becomes complex. *Nat. Rev. Mol. Cell Biol.* **7,** 678–689
3. Kopan, R., and Ilagan, M. X. (2009) The canonical Notch signaling pathway: unfolding the activation mechanism. *Cell* **137,** 216–233
4. Fortini, M. E. (2009) Notch signaling: the core pathway and its posttranslational regulation. *Dev. Cell* **16,** 633–647
5. Joutel, A., Corpechot, C., Ducros, A., Vahedi, K., Chabriat, H., Mouton, P., Alamowitch, S., Domenga, V., Cécillion, M., Marechal, E., Maciazek, J., Vayssiere, C., Cruaud, C., Cabanis, E. A., Ruchoux, M. M., Weissenbach, J., Bach, J. F., Bousser, M. G., and Tournier-Lasserve, E. (1996) Notch3 mutations in CADASIL, a hereditary adult-onset condition causing stroke and dementia. *Nature* **383,** 707–710
6. Gridley, T. (2003) Notch signaling and inherited disease syndromes. *Hum. Mol. Genet.* **12,** R9–R13
7. Weng, A. P., and Aster, J. C. (2004) Multiple niches for Notch in cancer: context is everything. *Curr. Opin. Genet. Dev.* **14,** 48–54
8. Moloney, D. J., Shair, L. H., Lu, F. M., Xia, J., Locke, R., Matta, K. L., and Haltiwanger, R. S. (2000) Mammalian Notch1 is modified with two unusual forms of *O*-linked glycosylation found on epidermal growth factor-like modules. *J. Biol. Chem.* **275,** 9604–9611
9. Whitworth, G. E., Zandberg, W. F., Clark, T., and Vocadlo, D. J. (2010) Mammalian Notch is modified by D-Xyl-α1–3-D-Xyl-α1–3-D-Glc-β1-*O*-Ser: implementation of a method to study *O*-glucosylation. *Glycobiology* **20,** 287–299
10. Matsuura, A., Ito, M., Sakaidani, Y., Kondo, T., Murakami, K., Furukawa, K., Nadano, D., Matsuda, T., and Okajima, T. (2008) *O*-Linked *N*-acetylglucosamine is present on the extracellular domain of Notch receptors. *J. Biol. Chem.* **283,** 35486–35495
11. Takeuchi, H., Fernández-Valdivia, R. C., Caswell, D. S., Nita-Lazar, A., Rana, N. A., Garner, T. P., Weldeghiorghis, T. K., Macnaughtan, M. A., Jafar-Nejad, H., and Haltiwanger, R. S. (2011) Rumi functions as both a protein *O*-glucosyltransferase and a protein *O*-xylosyltransferase. *Proc. Natl. Acad. Sci. U.S.A.* **108,** 16600–16605
12. Rana, N. A., Nita-Lazar, A., Takeuchi, H., Kakuda, S., Luther, K. B., and Haltiwanger, R. S. (2011) *O*-Glucose trisaccharide is present at high but variable stoichiometry at multiple sites on mouse Notch1. *J. Biol. Chem.* **286,** 31623–31637
13. Shao, L., Moloney, D. J., and Haltiwanger, R. (2003) Fringe modifies *O*-fucose on mouse Notch1 at epidermal growth factor-like repeats within the ligand-binding site and the Abruptex region. *J. Biol. Chem.* **278,** 7775–7782
14. Brückner, K., Perez, L., Clausen, H., and Cohen, S. (2000) Glycosyltransferase activity of Fringe modulates Notch-Delta interactions. *Nature* **406,** 411–415
15. Moloney, D. J., Panin, V. M., Johnston, S. H., Chen, J., Shao, L., Wilson, R., Wang, Y., Stanley, P., Irvine, K. D., Haltiwanger, R. S., and Vogt, T. F. (2000) Fringe is a glycosyltransferase that modifies Notch. *Nature* **406,** 369–375
16. Okajima, T., and Irvine, K. D. (2002) Regulation of notch signaling by *O*-linked fucose. *Cell* **111,** 893–904
17. Sasamura, T., Sasaki, N., Miyashita, F., Nakao, S., Ishikawa, H. O., Ito, M., Kitagawa, M., Harigaya, K., Spana, E., Bilder, D., Perrimon, N., and Matsuno, K. (2003) *Neurotic*, a novel maternal neurogenic gene, encodes an *O*-fucosyltransferase that is essential for Notch-Delta interactions. *Development* **130,** 4785–4795
18. Shi, S., and Stanley, P. (2003) Protein *O*-fucosyltransferase 1 is an essential component of Notch signaling pathways. *Proc. Natl. Acad. Sci. U.S.A.* **100,** 5234–5239
19. Fleming, R. J., Gu, Y., and Hukriede, N. A. (1997) Serrate-mediated activation of Notch is specifically blocked by the product of the gene *fringe* in the dorsal compartment of the *Drosophila* wing imaginal disc. *Development* **124,** 2973–2981
20. Panin, V. M., Papayannopoulos, V., Wilson, R., and Irvine, K. D. (1997) Fringe modulates Notch-ligand interactions. *Nature* **387,** 908–912
21. Hicks, C., Johnston, S. H., diSibio, G., Collazo, A., Vogt, T. F., and Weinmaster, G. (2000) Fringe differentially modulates Jagged1 and Delta1 signalling through Notch1 and Notch2. *Nat. Cell Biol.* **2,** 515–520
22. Haines, N., and Irvine, K. D. (2003) Glycosylation regulates Notch signal-

ling. *Nat. Rev. Mol. Cell Biol.* **4,** 786–797
23. Okajima, T., Xu, A., Lei, L., and Irvine, K. D. (2005) Chaperone activity of protein *O*-fucosyltransferase 1 promotes notch receptor folding. *Science* **307,** 1599–1603
24. Okajima, T., Reddy, B., Matsuda, T., and Irvine, K. D. (2008) Contributions of chaperone and glycosyltransferase activities of *O*-fucosyltransferase 1 to Notch signaling. *BMC Biol.* **6,** 1
25. Sasamura, T., Ishikawa, H. O., Sasaki, N., Higashi, S., Kanai, M., Nakao, S., Ayukawa, T., Aigaki, T., Noda, K., Miyoshi, E., Taniguchi, N., and Matsuno, K. (2007) The *O*-fucosyltransferase *O*-fut1 is an extracellular component that is essential for the constitutive endocytic trafficking of Notch in *Drosophila*. *Development* **134,** 1347–1356
26. Sasaki, N., Sasamura, T., Ishikawa, H. O., Kanai, M., Ueda, R., Saigo, K., and Matsuno, K. (2007) Polarized exocytosis and transcytosis of Notch during its apical localization in *Drosophila* epithelial cells. *Genes Cells* **12,** 89–103
27. Acar, M., Jafar-Nejad, H., Takeuchi, H., Rajan, A., Ibrani, D., Rana, N. A., Pan, H., Haltiwanger, R. S., and Bellen, H. J. (2008) Rumi is a CAP10 domain glycosyltransferase that modifies Notch and is required for Notch signaling. *Cell* **132,** 247–258
28. Leonardi, J., Fernandez-Valdivia, R., Li, Y. D., Simcox, A. A., and Jafar-Nejad, H. (2011) Multiple *O*-glucosylation sites on Notch function as a buffer against temperature-dependent loss of signaling. *Development* **138,** 3569–3578
29. Fernandez-Valdivia, R., Takeuchi, H., Samarghandi, A., Lopez, M., Leonardi, J., Haltiwanger, R. S., and Jafar-Nejad, H. (2011) Regulation of mammalian Notch signaling and embryonic development by the protein *O*-glucosyltransferase Rumi. *Development* **138,** 1925–1934
30. Lee, T. V., Sethi, M. K., Leonardi, J., Rana, N. A., Buettner, F. F., Haltiwanger, R. S., Bakker, H., and Jafar-Nejad, H. (2013) Negative regulation of notch signaling by xylose. *PLoS Genet.* **9,** e1003547
31. Irvine, K. D., and Wieschaus, E. (1994) fringe, a Boundary-specific signaling molecule, mediates interactions between dorsal and ventral cells during *Drosophila* wing development. *Cell* **79,** 595–606
32. Roos, C., Kolmer, M., Mattila, P., and Renkonen, R. (2002) Composition of *Drosophila melanogaster* proteome involved in fucosylated glycan metabolism. *J. Biol. Chem.* **277,** 3168–3175
33. Ayukawa, T., Matsumoto, K., Ishikawa, H. O., Ishio, A., Yamakawa, T., Aoyama, N., Suzuki, T., and Matsuno, K. (2012) Rescue of Notch signaling in cells incapable of GDP-L-fucose synthesis by gap junction transfer of GDP-L-fucose in *Drosophila*. *Proc. Natl. Acad. Sci. U.S.A.* **109,** 15318–15323
34. Fuerstenberg, S., and Giniger, E. (1998) Multiple roles for notch in *Drosophila* myogenesis. *Dev. Biol.* **201,** 66–77
35. Go, M. J., Eastman, D. S., and Artavanis-Tsakonas, S. (1998) Cell proliferation control by Notch signaling in *Drosophila* development. *Development* **125,** 2031–2040
36. Lloyd, T. E., Atkinson, R., Wu, M. N., Zhou, Y., Pennetta, G., and Bellen, H. J. (2002) Hrs regulates endosome membrane invagination and tyrosine kinase receptor signaling in *Drosophila*. *Cell* **108,** 261–269
37. Wilder, E. L., and Perrimon, N. (1995) Dual functions of *wingless* in the *Drosophila* leg imaginal disc. *Development* **121,** 477–488
38. Emery, G., Hutterer, A., Berdnik, D., Mayer, B., Wirtz-Peitz, F., Gaitan, M. G., and Knoblich, J. A. (2005) Asymmetric Rab 11 endosomes regulate delta recycling and specify cell fate in the *Drosophila* nervous system. *Cell* **122,** 763–773
39. Windler, S. L., and Bilder, D. (2010) Endocytic internalization routes required for delta/notch signaling. *Curr. Biol.* **20,** 538–543
40. Rong, Y. S., and Golic, K. G. (2000) Gene targeting by homologous recombination in *Drosophila*. *Science* **288,** 2013–2018
41. Gong, W. J., and Golic, K. G. (2003) Ends-out, or replacement, gene targeting in *Drosophila*. *Proc. Natl. Acad. Sci. U.S.A.* **100,** 2556–2561
42. Xu, T., and Rubin, G. M. (1993) Analysis of genetic mosaics in developing and adult *Drosophila* tissues. *Development* **117,** 1223–1237
43. Lee, T., and Luo, L. (2001) Mosaic analysis with a repressible cell marker (MARCM) for *Drosophila* neural development. *Trends Neurosci.* **24,** 251–254
44. Matsuno, K., Ito, M., Hori, K., Miyashita, F., Suzuki, S., Kishi, N., Artavanis-Tsakonas, S., and Okano, H. (2002) Involvement of a proline-rich motif and RING-H2 finger of Deltex in the regulation of Notch signaling. *Development* **129,** 1049–1059
45. Fehon, R. G., Kooh, P. J., Rebay, I., Regan, C. L., Xu, T., Muskavitch, M. A., and Artavanis-Tsakonas, S. (1990) Molecular interactions between the protein products of the neurogenic loci Notch and Delta, two EGF-homologous genes in *Drosophila*. *Cell* **61,** 523–534
46. Delgehyr, N., Wieland, U., Rangone, H., Pinson, X., Mao, G., Dzhindzhev, N. S., McLean, D., Riparbelli, M. G., Llamazares, S., Callaini, G., Gonzalez, C., and Glover, D. M. (2012) *Drosophila* Mgr, a Prefoldin subunit cooperating with von Hippel Lindau to regulate tubulin stability. *Proc. Natl. Acad. Sci. U.S.A.* **109,** 5729–5734
47. Diederich, R. J., Matsuno, K., Hing, H., and Artavanis-Tsakonas, S. (1994) Cytosolic interaction between deltex and Notch ankyrin repeats implicates deltex in the Notch signaling pathway. *Development* **120,** 473–481
48. Brook, W. J., and Cohen, S. M. (1996) Antagonistic interactions between wingless and decapentaplegic responsible for dorsal-ventral pattern in the *Drosophila* Leg. *Science* **273,** 1373–1377
49. Blochlinger, K., Bodmer, R., Jan, L. Y., and Jan, Y. N. (1990) Patterns of expression of cut, a protein required for external sensory organ development in wild-type and cut mutant *Drosophila* embryos. *Genes Dev.* **4,** 1322–1331
50. O'Neill, E. M., Rebay, I., Tjian, R., and Rubin, G. M. (1994) The activities of two Ets-related transcription factors required for *Drosophila* eye development are modulated by the Ras/MAPK pathway. *Cell* **78,** 137–147
51. Tanaka, T., and Nakamura, A. (2008) The endocytic pathway acts downstream of Oskar in *Drosophila* germ plasm assembly. *Development* **135,** 1107–1117
52. Yamakawa, T., Yamada, K., Sasamura, T., Nakazawa, N., Kanai, M., Suzuki, E., Fortini, M. E., and Matsuno, K. (2012) Deficient Notch signaling associated with neurogenic *pecanex* is compensated for by the unfolded protein response in *Drosophila*. *Development* **139,** 558–567
53. Nolo, R., Abbott, L. A., and Bellen, H. J. (2000) Senseless, a Zn finger transcription factor, is necessary and sufficient for sensory organ development in *Drosophila*. *Cell* **102,** 349–362
54. Culi, J., and Mann, R. S. (2003) Boca, an endoplasmic reticulum protein required for wingless signaling and trafficking of LDL receptor family members in *Drosophila*. *Cell* **112,** 343–354
55. Stahl, M., Uemura, K., Ge, C., Shi, S., Tashima, Y., and Stanley, P. (2008) Roles of Pofut1 and *O*-fucose in mammalian Notch signaling. *J. Biol. Chem.* **283,** 13638–13651
56. Lira-Navarrete, E., Valero-González, J., Villanueva, R., Martínez-Júlvez, M., Tejero, T., Merino, P., Panjikar, S., and Hurtado-Guerrero, R. (2011) Structural insights into the mechanism of protein *O*-fucosylation. *PLoS One* **6,** e25365
57. Rulifson, E. J., and Blair, S. S. (1995) Notch regulates wingless expression and is not required for reception of the paracrine wingless signal during wing margin neurogenesis in *Drosophila*. *Development* **121,** 2813–2824
58. Chou, T. B., and Perrimon, N. (1996) The autosomal FLP-DFS technique for generating germ line mosaics in *Drosophila melanogaster*. *Genetics* **144,** 1673–1679
59. Simpson, P. (1990) Lateral inhibition and the development of the sensory bristles of the adult peripheral nervous system of *Drosophila*. *Development* **109,** 509–519
60. Ishikawa, H. O., Higashi, S., Ayukawa, T., Sasamura, T., Kitagawa, M., Harigaya, K., Aoki, K., Ishida, N., Sanai, Y., and Matsuno, K. (2005) Notch deficiency implicated in the pathogenesis of congenital disorder of glycosylation IIc. *Proc. Natl. Acad. Sci. U.S.A.* **102,** 18532–18537
61. Tonetti, M., Sturla, L., Bisso, A., Zanardi, D., Benatti, U., and De Flora, A. (1998) The metabolism of 6-deoxyhexoses in bacterial and animal cells. *Biochimie* **80,** 923–931
62. Rauskolb, C., Correia, T., and Irvine, K. D. (1999) Fringe-dependent separation of dorsal and ventral cells in the *Drosophila* wing. *Nature* **401,** 476–480
63. Pitsouli, C., and Delidakis, C. (2005) The interplay between DSL proteins and ubiquitin ligases in Notch signaling. *Development* **132,** 4041–4050
64. Fehon, R. G., Johansen, K., Rebay, I., and Artavanis-Tsakonas, S. (1991) Complex cellular and subcellular regulation of notch expression during

embryonic and imaginal development of *Drosophila*: implications for notch function. *J. Cell Biol.* **113,** 657–669
65. Wang, W., and Struhl, G. (2004) *Drosophila* Epsin mediates a select endocytic pathway that DSL ligands must enter to activate Notch. *Development* **131,** 5367–5380
66. Glavic, A., López-Varea, A., and de Celis, J. F. (2011) The balance between GMD and OFUT1 regulates Notch signaling pathway activity by modulating Notch stability. *Biol. Res.* **44,** 25–34
67. Perdigoto, C. N., Schweisguth, F., and Bardin, A. J. (2011) Distinct levels of Notch activity for commitment and terminal differentiation of stem cells in the adult fly intestine. *Development* **138,** 4585–4595
68. Hiruma-Shimizu, K., Hosoguchi, K., Liu, Y., Fujitani, N., Ohta, T., Hinou, H., Matsushita, T., Shimizu, H., Feizi, T., and Nishimura, S. (2010) Chemical synthesis, folding, and structural insights into *O*-fucosylated epidermal growth factor-like repeat 12 of mouse Notch-1 receptor. *J. Am. Chem. Soc.* **132,** 14857–14865
69. Wang, Y., and Spellman, M. W. (1998) Purification and characterization of a GDP-fucose:polypeptide fucosyltransferase from Chinese hamster ovary cells. *J. Biol. Chem.* **273,** 8112–8118
70. Luo, Y., and Haltiwanger, R. S. (2005) *O*-Fucosylation of Notch occurs in the endoplasmic reticulum. *J. Biol. Chem.* **280,** 11289–11294
71. Takeuchi, H., Kantharia, J., Sethi, M. K., Bakker, H., and Haltiwanger, R. S. (2012) Site-specific *O*-glucosylation of the epidermal growth factor-like (EGF) repeats of notch: efficiency of glycosylation is affected by proper folding and amino acid sequence of individual EGF repeats. *J. Biol. Chem.* **287,** 33934–33944
72. Ge, C., and Stanley, P. (2008) The *O*-fucose glycan in the ligand-binding domain of Notch1 regulates embryogenesis and T cell development. *Proc. Natl. Acad. Sci. U.S.A.* **105,** 1539–1544
73. Moremen, K. W., Tiemeyer, M., and Nairn, A. V. (2012) Vertebrate protein glycosylation: diversity, synthesis and function. *Nat. Rev. Mol. Cell Biol.* **13,** 448–462